MODELING THE EFFECT OF SCR DENOX UNIT ON DIESEL ENGINE PERFORMANCE

A THESIS SUBMITTED TO
THE GRADUATE SCHOOL OF NATURAL AND APPLIED SCIENCES
OF
MIDDLE EAST TECHNICAL UNIVERSITY

BY

PELSU PELEN

IN PARTIAL FULFILLMENT OF THE REQUIREMENTS
FOR
THE DEGREE OF MASTER OF SCIENCE
IN
MECHANICAL ENGINEERING

JANUARY 2020

Approval of the thesis:

MODELING THE EFFECT OF SCR DENOX UNIT ON DIESEL ENGINE PERFORMANCE

submitted by **PELSU PELEN** in partial fulfillment of the requirements for the degree of **Master of Science in Mechanical Engineering Department, Middle East Technical University** by,

Prof. Dr. Halil Kalıpçılar
Dean, Graduate School of **Natural and Applied Sciences** ________________

Prof. Dr. M. A. Sahir Arıkan
Head of Department, **Mechanical Engineering** ________________

Assist. Prof. Dr. Feyza Kazanç Özerinç
Supervisor, **Mechanical Engineering, METU** ________________

Prof. Dr. Deniz Üner
Co-Supervisor, **Chemical Engineering, METU** ________________

Examining Committee Members:

Prof. Dr. Almıla Güvenç Yazıcıoğlu
Mechanical Engineering, METU ________________

Assist. Prof. Dr. Feyza Kazanç Özerinç
Mechanical Engineering, METU ________________

Prof. Dr. Deniz Üner
Chemical Engineering, METU ________________

Prof. Dr. Ahmet Yozgatlıgil
Mechanical Engineering, METU ________________

Assoc. Prof. Dr. Murat Kadri Aktaş
Mechanical Engineering, TOBB ________________

Date: 30.01.2020

I hereby declare that all information in this document has been obtained and presented in accordance with academic rules and ethical conduct. I also declare that, as required by these rules and conduct, I have fully cited and referenced all material and results that are not original to this work.

Name, Surname: Pelsu Pelen

Signature:

ABSTRACT

MODELING THE EFFECT OF SCR DENOX UNIT ON DIESEL ENGINE PERFORMANCE

Pelen, Pelsu
Master of Science, Mechanical Engineering
Supervisor: Assist. Prof. Dr. Feyza Kazanç Özerinç
Co-Supervisor: Prof. Dr. Deniz Üner

January 2020, 86 pages

The design of the internal combustion engines and the aftertreatment systems cannot be considered independently since imposing an aftertreatment equipment into the exhaust system brings extra backpressure which in turn decreases the engine efficiency and increases the fuel consumption and CO_2 emission. In the present study, the existing 3D monolith reactor model in COMSOL Multiphysics® applications is modified to account for an SCR deNO_x unit having 600 cpsi cell density by using exhaust mass flow rate and temperature data of a SCANIA 9-liter off-road Diesel engine. The model is verified against a published experimental work. While performing analyses, 98% NO_x conversion is aimed. Results showed that when the engine operates at 2100 rpm, 29.1 kPa backpressure is observed in the SCR deNO_x unit having 600 cpsi cell density and 20 cm diameter. It is seen that backpressure decreased down to 4.9 kPa by increasing the SCR deNO_x unit diameter to 25 cm. Furthermore, it is observed that 50% more backpressure is formed to obtain only 1% more NO_x conversion in the examined SCR deNO_x unit conditions. When the engine efficiency is considered, backpressure caused by SCR unit reduces the net work that can be obtained from the engine. If the engine compression ratio is increased to

enhance the net work, the efficiency increases however higher NO_x emission is observed due to higher temperatures arising from higher compression ratios.

Keywords: NOx Emission, Selective Catalytic Reduction, SCR, DeNOx, Aftertreatment System, Exhaust System, Pressure Drop in Monolith Channels, Exhaust Backpressure

ÖZ

SCR DENOX ÜNİTELERİNİN DİZEL MOTOR PERFORMANSINA ETKİSİNİN MODELLENMESİ

Pelen, Pelsu
Yüksek Lisans, Makina Mühendisliği
Tez Danışmanı: Dr. Öğr. Üyesi Feyza Kazanç Özerinç
Ortak Tez Danışmanı: Prof. Dr. Deniz Üner

Ocak 2020, 86 sayfa

İçten yanmalı motor ve egzoz sistemi tasarımları birbirinden bağımsız bir şekilde düşünülememektedir. Bunun sebebi, egzoz sistemi ekipmanlarının ters basınç sorununu beraberinde getirmesi ve bunun da motor verimliliğinde azalmaya, yakıt tüketimi ve CO_2 salınımında artmaya yol açmasıdır. Bu çalışmada, var olan COMSOL® üç boyutlu monolit reaktör uygulaması modifiye edilmiş ve 9 litre SCANIA arazi Dizel motoruna ait egzoz debi ve sıcaklık verileri kullanılarak 600 cpsi hücre yoğunluğuna sahip SCR deNO_x ünitesi oluşturulmuştur. Deneysel bir çalışmaya göre modelin verifikasyonu sağlanmıştır. Analizler sırasında %98 NO_x dönüşümü hedeflenmiştir. 2100 rpm motor hızında 600 cpsi hücre yoğunluğu ve 20 cm çapa sahip SCR deNO_x ünitesi için 29.1 kPa ters basınç saptanmıştır. SCR ünite çapı 25 cm'ye çıkarılarak analizler tekrarlandığında ters basıncın 4.9 kPa'a kadar gerilediği görülmüştür. Ayrıca, %1 fazla NO_x dönüşümü elde edebilmek için %50 daha fazla ters basınç gerçekleştiği gözlemlenmektedir. Motor verimliliği göz önüne alındığında, SCR'nin neden olduğu ters basıncın motordan elde edilen net işi azalttığı sonucuna ulaşılmıştır. Net işi arttırmak için motorun sıkıştırma oranı arttırılırsa, motor verimliliğinin arttığı ancak NO_x salınımında sıcaklık artışından kaynaklanan bir artış olduğu görülmektedir.

Anahtar Kelimeler: NOx Emisyonu, Seçici Katalitik İndirgeme, SCR, DeNOx, Egzoz Sistemi, Monolit Kanallarda Basınç Düşümü, Egzoz Sistemi Ters Basıncı

To my family

ACKNOWLEDGEMENTS

First of all, I would like to express sincere gratitude to my dear advisors Assist. Prof. Dr. Feyza Kazanç Özerinç and Prof. Dr. Deniz Üner for sparing their hours for this work and provide rapid progress with their accurate directions.

Secondly, I would like to thank my friends Sinan Şahin Candan, Ömer Faruk Önder, Sinem Uluocak, Talha Öz, Caner Güven, Ege Erdem, Eray Payaslıoğlu, Mehmet Furkan Söyleyici and Kaan Koçcaz who accompanied me during this exhaustive period, gave courage to complete thesis and were always by my side in the time of need.

Finally, I would like to thank my mother for her huge effort, understanding and simply being my biggest supporter in life.

TABLE OF CONTENTS

LIST OF TABLES

TABLES

LIST OF FIGURES

FIGURES

LIST OF ABBREVIATIONS

ASC	Ammonia Slip Catalyst
BDC	Bottom Dead Center
BP	Brake Power
BSFC	Brake Specific Fuel Consumption
bTDC	Before Top Dead Center
BTE	Brake Thermal Efficiency
CR	Compression Ratio
DEF	Diesel Exhaust Fluid
DOC	Diesel Oxidation Catalyst
DPF	Diesel Particulate Filter
EBP	Exhaust Backpressure
EGR	Exhaust Gas Recirculation
IP	Injection Pressure
IT	Injection Timing
LCV	Lower Calorific Value
LNT	Lean NO_x Trap
PV	Pressure-Volume
RGF	Residual Gas Fraction
SCR	Selective Catalytic Reduction
TDC	Top Dead Center
TWC	Three-Way Catalyst

LIST OF SYMBOLS

V_{TDC}	Cylinder volume at Top Dead Center (m^3)
V_{BDC}	Cylinder volume at Bottom Dead Center (m^3)
V_n	Cylinder volume at state n, n=1, 2, 3, 4 (m^3)
V_{cat}	Catalyst volume (m^3)
W_{cat}	Catalyst mass (kg)
$\dot{m}_{fuel}$	Mass flow rate of the fuel to the cylinder (kg/s)
$\dot{m}$	Mass flow rate of engine exhaust gas (kg/s)
N	Cell density (cell per square meter or cell per square inch)
a	Cell spacing (m)
D_h	Hydraulic diameter (m)
t	Supporting wall thickness (m)
L	Length of the monolith (m)
A	Open frontal area of the monolith (m^2)
κ	Permeability (m^2)
μ	Dynamic viscosity (Pa.s)
ρ	Fluid density (kg/m^3)
P	Pressure (Pa)
T	Temperature (K)
T_{amb}	Ambient temperature (K)
c_p	Heat capacity ($J/m^3.K$)

Q	Heat source due to reactions (W/m^3)
q’’	Convective heat flux (W/m^2)
k_{eq}	Equivalent thermal conductivity (W/m.K)
k_P	Conductivity of supporting walls (W/m.K)
k_L	Conductivity of the fluid (W/m.K)
$\bar{h}$	Average heat transfer coefficient (W/m^2.K)
$R_{external}$	External mass transfer resistance (s/m)
$R_{internal}$	Internal mass transfer resistance (s/m)
$R_{reaction}$	Reaction resistance (s/m)
R_{total}	Total resistance (s/m)
Sh	Sherwood number (1)
$d_{\Omega 1}$	Transverse diffusion length (m)
$d_{\Omega 2}$	Transverse diffusion length in washcoat (m)
$P_{\Omega 1}$	Washcoat-fluid interface perimeter (m)
$A_{\Omega 1}$	Channel cross-sectional area (m^2)
$A_{\Omega 2}$	Washcoat cross-sectional area (m^2)
D_i	Diffusivity of species i (m^2/s)
D_e	Effective diffusivity in washcoat (m^2/s)
Φ	Thiele modulus
r'_{NO}	Reaction rate of NO in mass basis (mol/kg.s)
r_{NO}	Reaction rate of NO in volume basis (mol/m^3.s)

k	Reaction rate constant (1/s)
F_{NOj}	Molar flow rate at j, j=i for inlet, j=e for exit (mol/s)
c_{NOj}	Molar concentration of NO at j, j=i for inlet, j=e for exit (mol/m^3.s)
υ_0	Volumetric flow rate (m^3/s)
SV	Space velocity (1/s)
τ	Space time (s)
r_v	Compression ratio
r_v'	Change in compression ratio
r_c	Cut-off ratio

CHAPTER 1

INTRODUCTION

1.1. Background Information

1.1.1. NO_x Emission

Although low concentration of nitrogen oxides (NO_x) are present in the ambient air due to nature events such as volcanic eruptions, main NO_x sources are human-driven activities. NO_x is mainly formed during the combustion of the fossil fuels, including fuel oil, natural gas and coal which are currently the primary energy sources around the world [1]. There are both stationary and mobile combustion sources emitting NO_x [6]. Industrial power plants are classified as stationary sources for NO_x emissions whereas Diesel, gasoline and jet engines used in land and air vehicles such as automobiles, trucks, ships, locomotives, airplanes are classified as mobile sources. NO_x term in NO_x emission studies refers to nitric oxide (NO) and nitrogen dioxide (NO_2) mostly [7]. When the typical distribution of NO_x emissions is considered, it is observed that NO emission forms 95% of total NO_x emissions from combustion sources whereas NO_2 emission forms only 5% [8]. This high NO emission amount influenced the focus of the present study.

There are three main NO_x formation means. The first is the thermal NO_x formation, which is the most common NO_x source in Diesel engines. In this type of formation oxygen and nitrogen in the supplied air react with each other. The global reaction describing thermal NO_x formation is

$$O_2 + N_2 \rightleftharpoons 2NO \qquad (1)$$

Zeldovich mechanism, which has been introduced by Zeldovich in 1946, describes the thermal NO_x formation in more details [8, 16]. Three reversible reactions in the extended Zeldovich mechanism are [8]

$$O + N_2 \rightleftarrows NO + N \qquad (2)$$

$$N + O_2 \rightleftarrows NO + O \qquad (3)$$

$$N + OH \rightleftarrows NO + H \qquad (4)$$

Equation (2) is the rate limiting step due to its high activation energy. The reason behind the high activation energy is the strong N_2 bond which needs to be broken for forward reaction to proceed [8]

The formation rate of NO can be described as in Equation 5 by using reactions (2), (3) and (4) in the extended Zeldovich mechanism;

$$\frac{d[NO]}{dt} = k_{1f}[O][N_2] + k_{2f}[N][O_2] + k_{3f}[N][OH] - k_{1r}[NO][N] - k_{2r}[NO][O] - k_{1r}[NO][H] \qquad (5)$$

Rate constant expressions of (2), (3) and (4) based on the work of Hanson et al [38].are listed in Table 1.1. k_{1f}, k_{2f} and k_{3f} represent the constant of forward reactions whereas k_{1r}, k_{2r} and k_{3r} represent reverse ones.

Table 1.1. Rate constants of forward and reverse reactions in extended Zeldovich mechanism [38]

Rate Constant Expression (m^3/mol.s)	
k_{1f}	$1.8 \times 10^8\ e^{-38370/T}$
k_{1r}	$3.8 \times 10^7\ e^{-425/T}$
k_{2f}	$1.8 \times 10^4\ T\ e^{-4860/T}$
k_{2r}	$3.8 \times 10^3\ T\ e^{-20820/T}$
k_{1f}	$7.1 \times 10^7\ e^{-450/T}$
k_{1r}	$1.7 \times 10^8\ e^{-24560/T}$

The time that is spent by combustion gases (residence time) in high temperature zones and oxygen amount presented in these zones are the other drivers for the thermal NO_x

formation. However, temperature reached in the combustion systems is the most significant parameter for the thermal NO_x formation. As it is observed in Figure 1.1, the most significant amount of NO_x emission due to thermal NO_x formation occurs in the temperature range of 1850°C-2000°C. Another NO_x formation mean is the fuel NO_x formation which occurs when the nitrogen bond in the fuel is broken. Lastly, NO_x is likely to be formed by the reaction of nitrogen with the intermediate products in prompt NO_x formation however this formation type constitutes the lowest amount compared to other two means [8, 16].

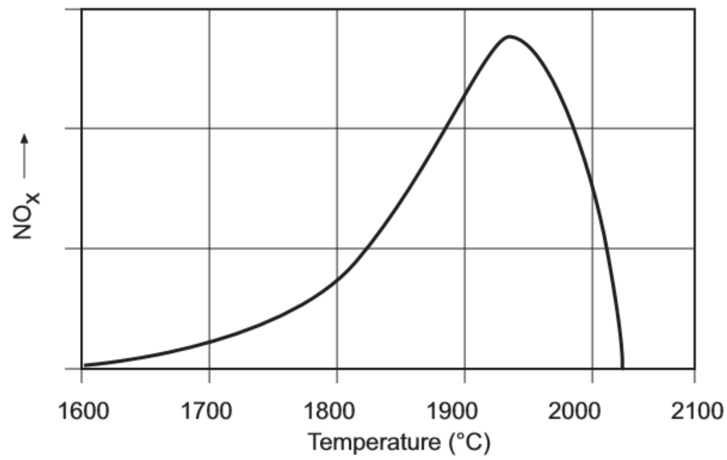

Figure 1.1. Relation between temperature and thermal NO_x formation [8]

Diesel engines mostly operate with compression ratios in the range of 14-21 [17]. Higher compression ratios compared to gasoline engines provide better thermal efficiency however result in higher temperatures reached in the cylinder and therefore cause more NO_x emission. Moreover, lean condition in Diesel engines aggravate the control of NO_x emission thus different remediation methods are required compared to gasoline engine [40].

NO_x emission is also proportional to the engine load therefore NO_x emissions are relatively low during engine start and warmup. Additionally, NO_x emission is higher in low engine speed since the residence time of the combustion gases in high temperature zones increases and results in NO_x formation incremental [16].

The global aim is to decrease NO_x emission caused by combustion sources since this type of emissions form the significant part of the global air pollution [1]. Nitrogen oxide emissions mostly have the form of NO that can react with atmospheric radicals and ozone easily resulting in NO_2 formation which is a toxic chemical. Emission of nitrogen oxides causes numerous hazards on both environment and human health [5]. Respiratory problems in humans such as lung diseases, lung cancer, asthma are triggered by exposure to nitrogen oxides. Moreover, heart diseases are also provoked by the nitrogen oxide exposures. The exposure is mostly via ingestion and inhalation. The dermal contact is also an exposure route however it consists of the minor part of the entire exposure [6].

In addition, sun light provokes the ozone formation by reactions involving volatile organic compounds and NO_2 in troposphere layer which again have negative impacts. Although the ozone layer traps the ultraviolet sunlight and therefore it is beneficial, ozone presenting in lower atmospheric layers are undesired since it is harmful for environment and human health [39].

1.1.2. NO_x Emission Regulations

In scope of mobile NO_x emission sources, 90% of global vehicle sales occur in G-20 countries and 17 of these countries (including Turkey) adopt European emission regulations. These regulations consist of stages containing increasingly stringent emission targets.

Diesel engines are subjected to more elaborative analyses since the NO_x emission is higher in these engine types due to higher temperatures reached in the engine cylinders compared to gasoline engines during engine operation.

Classification of the engine directly affects the type of EU regulation applied. Euro I, Euro II, Euro III, Euro IV, Euro V and Euro VI standards are implemented in on-road vehicles that consist of light-duty (passenger cars, light commercial vehicles) and heavy-duty vehicles (buses, heavy trucks). Unlike the on-road vehicles, Stage I, Stage II, Stage III, Stage IV and Stage V standards are used in off-road vehicles such as construction vehicles, forklift trucks, mobile cranes, snowplows, tractors etc. Euro VI and Stage V are the latest ones among all these standards.

In North America, Korea and Japan, "Tier" term is utilized in emission standards instead of "Euro" and "Stage" terms. These terms are comparable with each other. For instance, Stage IV and Tier 4f point similar emission targets [9, 10].

Table 1.2 reveals the variation in NO_x emission limits in time for passenger cars that are under light duty vehicles category. It is observed that NO_x emission target in Euro VI standard is 56% less than Euro V and 84% less than Euro III. For heavy duty vehicles, again a large reduction in NO_x emission limit is observed from Euro V to Euro VI, from 2.0 g/kWh to 0.4 g/kWh (in steady-state testing) which is equal to 80% reduction [12].

Table 1.2. EU emission standards for passenger cars having Diesel engine [9]

EU Standard	NO_x Emission Limit (g/km)	Year Introduced
Euro I	-	1992
Euro II	-	1997
Euro III	0.50	2001
Euro IV	0.25	2006
Euro V	0.18	2011
Euro VI	0.08	2016

The Commission under European Council have proposed Euro VI standard recognizing that Euro VI will affect the advantages in fuel consumption and CO and

HC emissions adversely. It has been stated that stringent NO_x emission requirements would provide a long-term precaution for automotive companies which intent to keep following Diesel technology [12]. The significant reduction values represented in Table 1.2 raise the importance of integrating efficient emission control equipment to aftertreatment systems.

1.1.3. Aftertreatment Systems

Recently, there are two means of emission control commonly used. These are managing the operational parameters in combustion and employing aftertreatment equipment to the exhaust system [16]. Due to increasingly stringent emission limits, advanced aftertreatment systems should be imposed to modern on-road and off-road vehicles. Modern aftertreatment systems integrated after Diesel engines may contain combination of some equipment such as Diesel oxidation catalyst (DOC), Diesel particulate filter (DPF), lean NO_x trap (LNT), selective catalytic reduction (SCR) unit, silencer etc. Each of these equipment has a different role in the exhaust system. (See Figure 1.2)

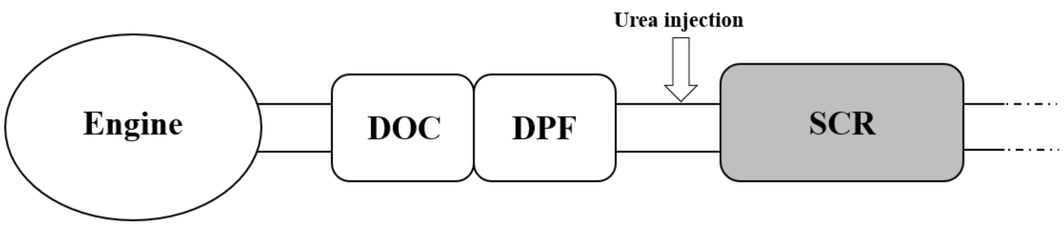

Figure 1.2. A commonly used Diesel engine aftertreatment setup

DOC provides CO and HC oxidation and convert these exhaust gases to harmless CO_2 and H_2O gases. Besides, it oxidizes the NO to NO_2 and enhance the fast SCR reaction in the SCR deNO_x unit. Filtration of the particulates from the exhaust gas is provided by DPF. Moreover, silencer may be required to decrease the noise of the exhaust gas and ensures that exhaust gases to reach the atmosphere under appropriate noise limits [17].

SCR and LNT units are used for deNO_x activities in market currently. In LNT (also called NO_x Storage and Reduction (NSR)), which is the first commercial lean deNO_x method implemented, NO_x molecules are stored at lean period then the medium is switched to rich and NO_x is discharged and converted to N_2 [17, 18].

In SCR approach, which is the focus of this study, NO_x is converted to N_2 with a reducing agent under lean conditions. The urea/water solution is the most common reducing agent used for this application and integrated to the vehicle as Diesel exhaust fluid (DEF) system. DEF is called "AdBlue" in European applications. The reducing agent is injected to the engine exhaust gas before it enters the SCR deNOx unit [17, 18]. In gasoline engines, three-way catalysts (TWC) has been used more than 30 years and provide 99% NO_x conversion. In these catalysts, NO_x is reduced by CO and HC. However, a TWC can only operate under stoichiometric conditions which does not work with the exhaust of Diesel engines. Therefore, lean Diesel exhaust conditions require other techniques such as SCR and LNT. Recently, SCR is the most effective method for the lean Diesel conditions [40]. Employing SCR and LNT units to the vehicles is an effective method to convert NO_x emitted from Diesel engines however those methods bring cost and weight penalty to the vehicles.

As it is mentioned in the first paragraph of this section, managing the operational parameters in combustion can be also used to decrease NO_x emission. In the exhaust gas recirculation (EGR) method, some of the exhaust gas is returned to the engine inlet and enters the cylinder again. EGR method provides decrease in cylinder temperature and therefore reduction in NO_x emission [25]. However, EGR cannot be enough to achieve the latest strict NO_x limits without the help of LNT or SCR aftertreatment units.

1.2. Motivation

In recent years, complying NO_x emission requirements that are declared in international standards have become more difficult. This issue is more critical in Diesel engines due to higher temperatures reached in engine cylinders during engine operation that triggers thermal NO_x formation. SCR units provide deNO_x activities however lead to extra backpressure and therefore may reduce the engine performance and increase the fuel consumption and CO_2 emission. To compensate this reduction in engine performance, designing the engine with a higher compression ratio can be a method regarding its other advantages such as lower fuel consumption and CO_2 emission. However, compression ratio increase results in increase in amount of NO_x released in turn. Therefore, the engine and its exhaust system shall be designed in line with each other regarding the backpressure caused by the exhaust system, engine efficiency and the emission limits in the latest standards. Figure 1.3 summarizes the relation between NO_x emission, pressure drop caused by SCR and engine performance.

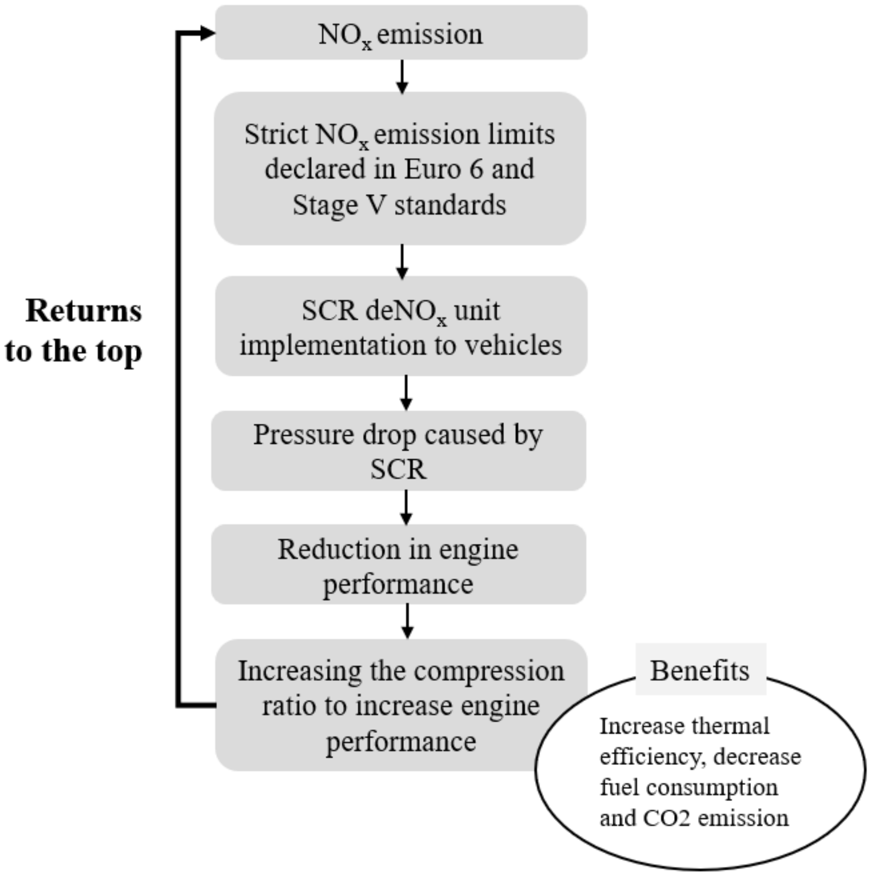

Figure 1.3. Relation between NO_x emission, backpressure caused by SCR and engine performance

1.3. Objectives

Present work investigates the effect of backpressure caused by SCR deNO_x unit on Diesel engine performance.

The main objectives of the work are as follows:

- Developing a model by using COMSOL Multiphysics® to compute the backpressure along a 600 cpsi deNO_x unit
- Obtaining the position where 98% NO_x conversion achieved in the model
- Running model at different SCR diameters
- Obtaining the effect of inlet temperature on conversion in SCR deNO_x unit

- Understanding the effect of the backpressure on thermal efficiency of the Diesel engine
- Examining the effect of compression ratio on engine parameters which are brake specific fuel consumption, brake thermal efficiency, CO_2 emission, NO_x emission.

CHAPTER 2

LITERATURE REVIEW

2.1. Selective Catalytic Reduction (SCR) Unit

In SCR, which is the most effective deNO$_x$ aftertreatment method used along with Diesel engines today, NO$_x$ is converted to N_2 and H_2O, which are harmless matters, with a reducing agent under lean conditions. Ammonia (NH_3) is used as the reducing agent and mostly stored in the form of urea/water solution in vehicles. The reducing agent is injected to the engine exhaust gas before it enters the SCR deNO$_x$ unit [17, 18].

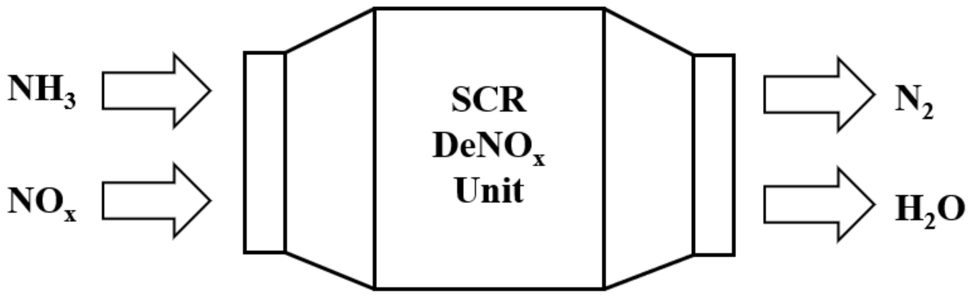

Figure 2.1. NO_x conversion into N_2 and H_2O by using NH_3 as the reducing agent in an SCR unit

2.1.1. Geometry of the SCR Unit

The geometry of the SCR unit consists of a honeycomb structure, which is constructed by repetition of the reactive channels. (See Figure 2.2) The supports separating reactive channels are made of ceramic or metallic materials. There are two means to manufacture a catalyst element. In the first one, honeycomb structure directly has the characteristic of a catalyst itself whereas in the second one the reactive channels in the honeycomb are washcoated with a catalyst layer. The most common catalyst types present in the market are precious metals (Pt etc.), metal oxides (V_2O_5 - TiO_2 etc.) and metal-exchanged zeolites (Cu-zeolite, Fe-zeolite etc.) [19].

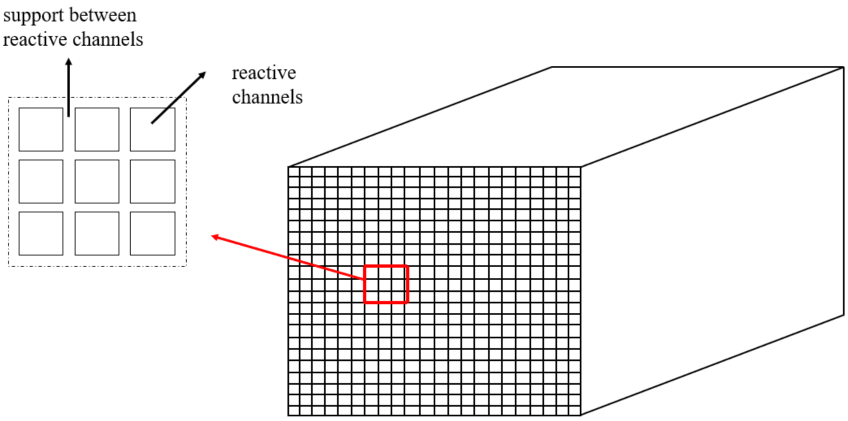

Figure 2.2. Representation of a square monolith

In power plant SCR units, square monoliths are used, which have cell density less than 46 cpsi (cell per square inch) In Figure 2.2, a square monolith is represented. On the other hand, round-shaped monoliths (with mostly cell densities with 25 – 900 cpsi) are used in automotive applications. Today, automotive SCR units commonly have 300 or 400 cpsi cell density. However, Heibel et al. [42] reported that 600 cpsi monoliths react 35% faster than 400 cpsi ones. Therefore, it is also important to assess the conversion and pressure drop performance of 600 cpsi monoliths. In heavy duty vehicles, monoliths with diameters up to 38 cm are used [40].

SCR unit performance can be measured by monitoring the NO_x content at the inlet and outlet and calculating how much NO_x is converted to N_2 and H_2O along the monolith unit. Theoretically, SCR units can be designed for deNO_x up close to 100% NO_x conversion [21, 22].

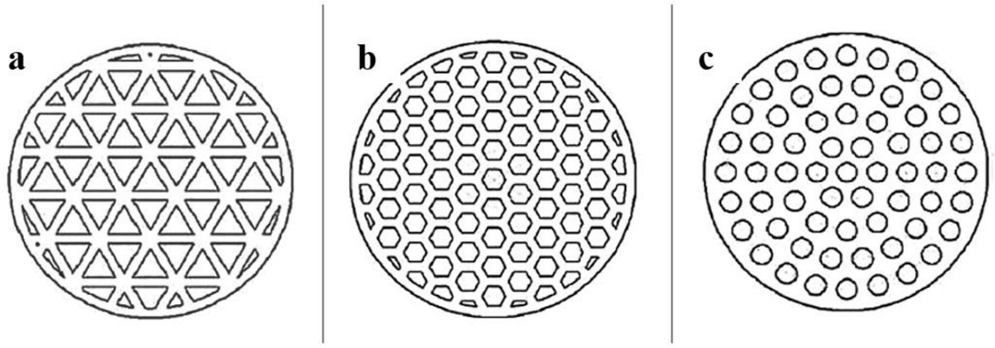

Figure 2.3. Various channel arrangements in a monolith. a.Triangular channels b.Hexagonal channels c. Circular channels [23]

Washcoated catalyst type, inlet NO_x concentration, operating temperature, geometry (cell density, channel shape and arrangement etc.) and ammonia slip are the parameters that affect the SCR deNO_x unit performance [21, 22]. Figure 2.3 represents the different channel arrangements for a cylindrical monolith.

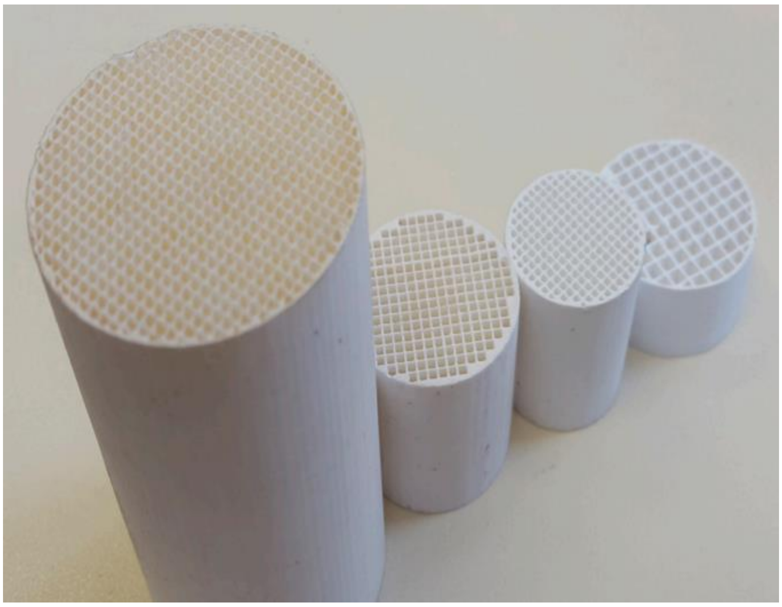

Figure 2.4. Ceramic monoliths at various diameters, lengths and cell densities [35]

Monoliths are sized according to need of NO_x conversion while regarding the constraints such as inlet temperature and maximum recommended pressure drop. Figure 2.4 indicates monoliths designed with different diameters and lengths due to varying conversion needs and constraints.

2.1.2. Pressure Drop in the SCR Unit

There are different approaches in literature to calculate pressure drop in SCR units. These approaches are directly related to the channel and flow characteristics. Hagen-Poiseuille pressure drop expression defined for a fully developed laminar flow through a circular channel can be found in any basic fluid mechanics textbook such as Fox et al [52]. Likewise, the pressure drop relation for a fully developed laminar flow through a square channel can be accessed easily. There are other available approaches that are capable of describing different flow characteristics. For instance, Hawthorn et al. [53] defined an expression that can take into account the entrance effects in a circular channel. Additionally, Shah et al. [54] reported a formula that can describe developing flow in a rectangular channel. Abu-Khiran et al. [55] compared all these approaches with an experimental study and the trend indicated in Figure 2.5 was stated for the laminar flow along the channel direction. This trend is separated into two regimes. In the first regime, boundary layer development is effective whereas fully developed laminar flow is observed in the second.

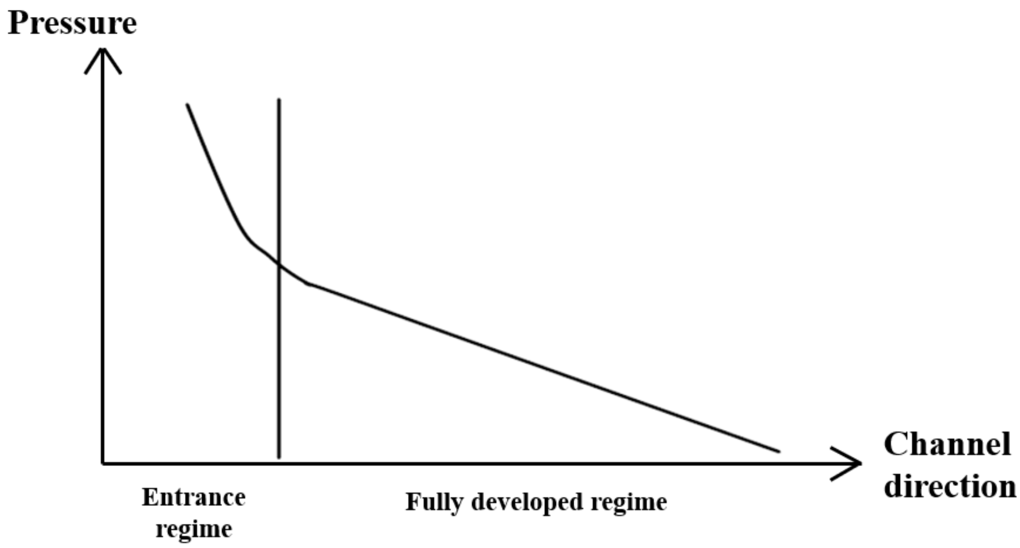

Figure 2.5. Laminar flow pressure profile along the channel direction [55] Copyright © 2003 SAE International, Copyright © 2003 Society of Automotive Engineers of Japan, Inc.

As it is stated in Section 2.1.1, the honeycomb structure of the SCR unit consists of thousands of reactive channels. Permeability term, which is defined as the ability of transmitting the flow, is important in monolith modeling since assigning the proper permeability value to the medium is much easier than performing calculations for thousands of channels. Darcy Law can be used to describe the relation between flow, permeability and pressure drop [32].

2.1.3. NO_x Conversion in the SCR Unit

Before the introduction of latest Euro 6 standard, even 60% - 80% NO_x conversion was sufficient to achieve Euro 4 and Euro 5 emission targets [41]. However, implementation of latest Euro 6 and Stage V emission regulations for on-road and off-road vehicles respectively have raised the issue of higher conversion needs. Reported SCR conversion efficiencies are around 90% which states a very high level of NO_x conversion compared to other aftertreatment NO_x reduction techniques [41]. Stanton et al. [43] stated that exhaust gas recirculation (EGR) can be eliminated when SCR NO_x conversion values exceed 98%. EGR elimination provides weight, space and cost saving. Additionally, complexity of the system reduces by removing EGR. Besides, Roberts et al. [44] reported that emission control methods including SCR should achieve at least 97-98% to meet the most cost-effective targets. As a result, in order to obtain the optimum balance considering the conversion efficiency, system cost and fuel consumption, 98+ % SCR is required [40]. Therefore, this value is used as the design driver in the present work to compute the length and pressure drop.

2.1.3.1. Chemical Kinetics in the SCR Unit

A number of reactions occur in the SCR deNO$_x$ unit in which the NO$_x$ is converted to harmless N_2 and H_2O compounds. The "standard SCR reaction" shown in equation (6) occurring in the SCR unit is equimolar in terms of NH_3 and NO and also involves O_2 as a reactant [40].

$$4NH_3 + 4NO + O_2 \longrightarrow 4N_2 + 6H_2O \qquad (6)$$

"fast SCR reaction" shown in equation (7) occurs when there is sufficient amount of NO_2 in the medium. Diesel oxidation catalyst (DOC) is used mostly to oxidize NO to produce NO_2 as in equation (8) to enhance the fast SCR [40].

$$2NH_3 + NO + NO_2 \longrightarrow 2N_2 + 3H_2O \qquad (7)$$

$$2NO + O_2 \longrightarrow 2NO_2 \qquad (8)$$

In the presence of excessive NO_2 amount produced by DOC, the reaction shown in equation (9) takes place. This case is not desired since some of the ammonia (NH_3) is consumed in (9) and (10) whereas the ammonia is actually supposed to be used to reduce NO. Additionally, the excess NO_2 can react with NH_3 and produce N_2O as shown in equation (10), which is another nitrogen oxide and an undesired chemical in the atmosphere [40].

$$8NH_3 + 6NO_2 \longrightarrow 7N_2 + 12H_2O \qquad (9)$$

$$2NH_3 + 2NO_2 \longrightarrow N_2 + N_2O + 3H_2O \qquad (10)$$

Ammonia oxidation (11), which is a side reaction, and SCR reaction compete in the SCR unit. This case is not desired since the some of the ammonia (NH_3) is consumed in (11) whereas the ammonia is actually supposed to be used to reduce NO.

$$4NH_3 + 3O_2 \longrightarrow 2N_2 + 6H_2O \qquad (11)$$

Furthermore, ammonia slip, which means ammonia passes through the SCR unit without reacting with any other compound, occurs if there is excess ammonia in the medium. An ammonia slip catalyst (ASC) can be used to minimize the ammonia slip [40].

2.2. Diesel Engine

Operational principle of an internal combustion engine is to convert the chemical energy bounded in the fuel into the mechanical energy. The Diesel engine, also called compression-ignition engine, is an internal combustion engine in which air is allowed to the cylinder first and compressed, then the fuel is injected and ignition takes place. In Diesel engines, the ignition occurs after compression and fuel injection instead of applying a spark-plug as in gasoline engines.

Since the risk of knocking is eliminated in Diesel engines due to the absence of flame propagation, higher compression ratios can be achieved. The limit of compression is predetermined by maximum allowable cylinder pressure instead of knocking which is a predetermining factor of compression ratio in gasoline engines [17]. Higher compression ratio provides higher net work therefore results in higher efficiency however in turn triggers the thermal NO_x formation causing higher NO_x emissions due to higher temperature zones formed in the cylinder.

2.2.1. Exhaust Gas Parameters in Diesel Engine

As engine speed and torque change due to vehicle speed, acceleration, road roughness or road slope, both mass flow rate and emission of NO_x, CO_2, HC at the engine exit vary [15]. Heavy duty engines have higher engine sizes and power outputs. On the other hand, higher emissions are observed for these engines. Table 2.1 indicates the SCANIA off-road engine sizes and their powers.

Table 2.1. Size and power range of SCANIA industrial engines

SCANIA Industrial Engines [37]			
	9 liters	**13 liters**	**16 liters**
Power Output	202-294 kW	257-405 kW	368-566 kW

EU emission regulations impose Stage I, II, III, IV and V emission standards for off-road vehicles. Stage IV and V standards address 0.4 g/kWh NO_x emission target, which is very stringent, for the engines with power output in the range of 130 - 560 kW [9]. SCANIA industrial engines seen in Table 2.1 fall into this group therefore they are imposed to stringent 0.4 g/kWh NO_x emission target. Since the target of 0.4 g/kWh NO_x has been introduced with the standard Stage IV, NO_x aftertreatment systems have been employed to the vehicles.

There is a maximum recommended pressure drop, which is defined by engine manufacturer, for every aftertreatment system because it is very important for the exhaust system to be consistent with the engine. This pressure drop values should not be exceeded, otherwise power loss and fuel consumption can reach undesirable levels. As an example of maximum recommended pressure drop, SCANIA DC09 312 industrial engine is given in Table 2.2. The value in the table is recommended for the entire aftertreatment system including pipes, DPF and SCR unit.

Table 2.2. Maximum recommended pressure drop of SCANIA DC09 312 industrial engine [10]

Engine Type	**Power Output**	**Standard to comply**	**Max Recommended Pressure Drop for the complete exhaust system**
DC09 312	202 kW	EU Stage V	26500 Pa

A 9-liter SCANIA industrial engine data represent that the engine exhaust mass flow rate increases when the engine speed increases. (See Figure 2.6) Higher exhaust mass flow rate means higher amount of gas is emitted from the engine in unit time. In addition, engine load impacts the Diesel emissions. Vasudeva et al. [29] showed that NO_x, CO, CO_2 and HC emissions increase with the increasing engine load.

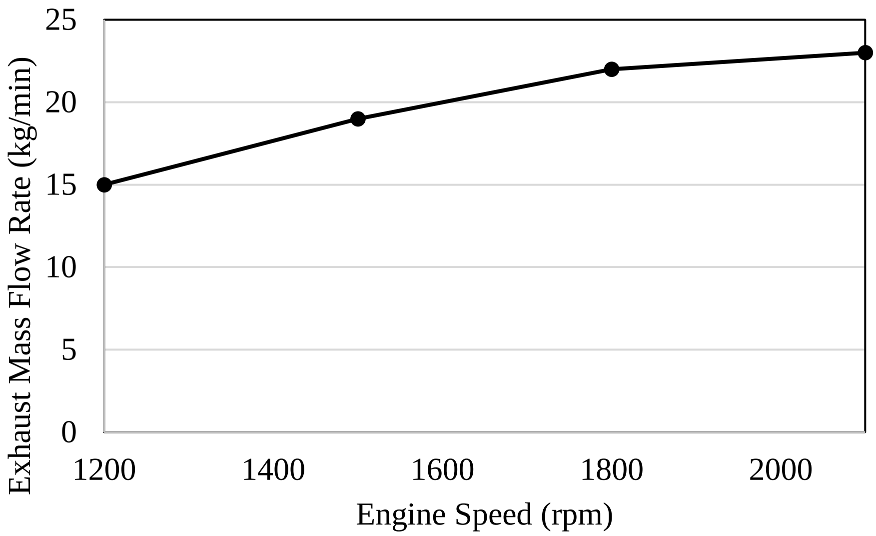

Figure 2.6. Exhaust mass flow rate data of a 9-liter SCANIA industrial engine varying with the engine speed [10].

Although aftertreatment system equipment (DOC, DPF, SCR, LNT, silencer etc.) in vehicles provide control on emission and noise, they yield pressure drop throughout the exhaust system. Therefore, pressure of the gas exhausted from the engine has to be at a level that allows exhaust gas to overcome the pressure drop along the exhaust system and reach the exit. If the engine exhaust gas discharged to the atmosphere directly in the absence of the aftertreatment system, engine exhaust pressure would be equivalent to atmospheric pressure. However, in real cases, an appropriate aftertreatment system is integrated to the vehicle complying the emission and noise targets therefore pressure at engine exhaust needs to be equal to the pressure drop caused by the exhaust system. Increased pressure drop is a very important challenge to overcome since it causes engine power loss and fuel consumption increase. Typically, 300 W of power is lost per 1 kPa of pressure drop [14].

Previously pellet-formed units had been used which caused much higher pressure drop values. Currently, they are replaced with the honeycomb monolith structure due to lower pressure drop with higher open frontal area [14].

2.2.2. Performance Parameters in Diesel Engine

As it is mentioned in Section 2.2, knocking risk is removed in Diesel engines therefore higher compression ratios (CR) can be achieved. Diesel engine CRs are normally in the range of 14 – 21. (whereas gasoline engines' compression ratio is in the range of 8 – 12 limited by knocking) [17].

CR in engines is defined as [26]

$$CR = \frac{V_{BDC} - V_{TDC}}{V_{TDC}} \qquad (12)$$

Where V_{BDC} are V_{TDC} the volumes of the engine cylinder when piston is at the bottom dead center (BDC) and the top dead center (TDC) positions respectively. (See Figure 2.7)

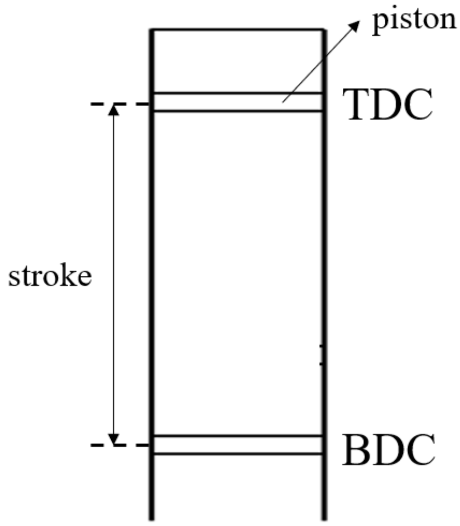

Figure 2.7. Positions of top dead center (TDC) and bottom dead center (BDC) on an engine cylinder

Diesel engines are distinguished from gasoline engines with their lower fuel consumption and higher thermal efficiencies. In this manner, the following two engine parameters are investigated in the present work:

- brake specific fuel consumption (BSFC)
- brake thermal efficiency (BTE)

BSFC basically represents the fuel consumed for the unit brake power (BP). It is defined as [26]

$$BSFC = \frac{\dot{m}_{fuel}}{BP} \tag{13}$$

where BP indicates the brake power produced by the engine at the shaft (kW) and $\dot{m}_{fuel}$ is mass flow rate of the fuel (kg/s).

BTE can be obtained by taking the reciprocal of the multiplication of BSFC and the fuel lower calorific value (LCV). It basically represents the engine thermal efficiency.

$$BTE = \frac{BP}{(\dot{m}_{fuel})(LCV)} = \frac{1}{(BSFC)(LCV)} \qquad (14)$$

In the present work, BSFC and BTE parameters are investigated and their relation with compression ratio is obtained. The aim is to then make a connection with the backpressure caused by SCR $deNO_x$ unit. It is expected that increase in CR is likely to compensate the engine performance loss caused by the backpressure.

2.2.2.1. Compression Ratio Effect on Brake Specific Fuel Consumption

There is a global trend aiming to minimize the fuel consumption in on-road and off-road vehicles in order to increase the cost efficiency of both gasoline and Diesel engine systems and save natural resources. Diesel engines have lower fuel consumption compared to gasoline engines.

Results from various published work are collected and plotted in Figure 2.8 in order to observe the effect of CR on BSFC for Diesel engines. The labels include fuel type and engine load parameters. There are other parameters that have impact on the curves of figure such as fuel injection pressure (IP) and injection timing (IT) however those parameters cannot be fully declared in the published studies therefore are not involved in the labels directly. All the curves have a decrease trend with increasing compression ratio even if different fuel type, engine load, fuel injection pressure or injection timing are used [27 - 30].

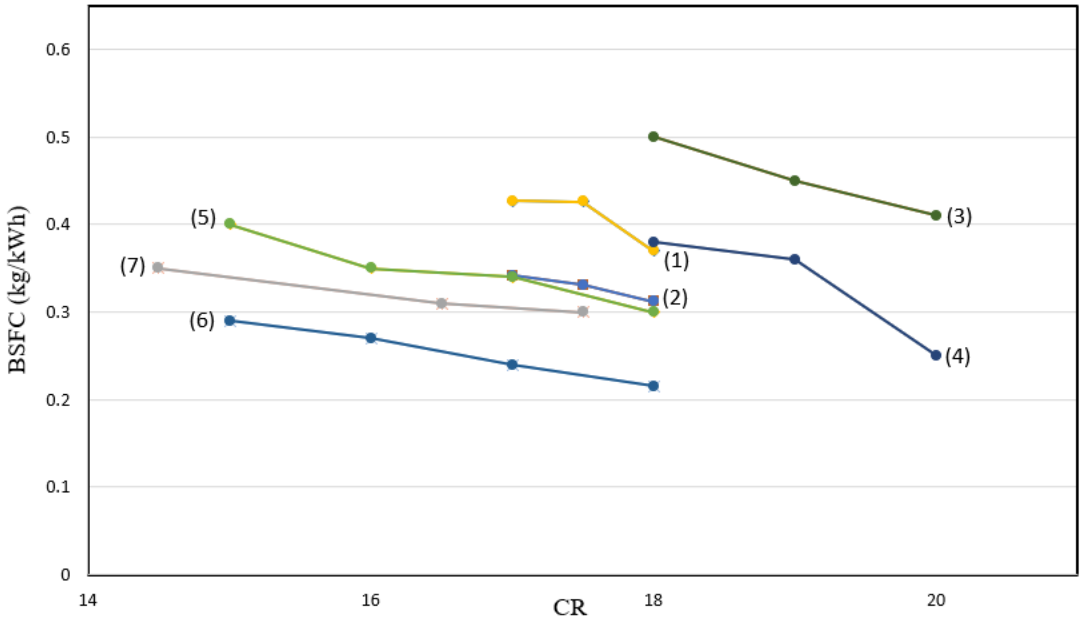

Legends of Figure 2.8.	(1)	(2)	(3)	(4)	(5)	(6)	(7)
Engine power (kW)	3.7	3.7	9	9	3.75	3.75	3.78
# of cylinder	1	1	1	1	1	1	1
# of stroke	4	4	4	4	4	4	4
Bore (mm)	80	80	76.2	76.2	87.5	87.5	80
Stroke (mm)	110	110	111.1	111.1	110	110	110
Speed (rpm)	1500	1500	1500	1500	1500	1500	1500
IT (°)	-	-	35-45 bTDC	35-45 bTDC	23 bTDC	23 bTDC	27 bTDC
IP (bar)	-	-	-	-	195	195	190
Fuel	Ethanol E20	Diesel	Diesel	Diesel	Diesel	Diesel	Diesel
Load (%)	50	50	50	100	60	100	100
Reference	[27]	[27]	[28]	[28]	[29]	[29]	[30]

Figure 2.8. BSFC variation with compression ratio

Kurre et al. [27] investigated the effect of CR values 17, 17.5 and 18 on BSFC by using a single cylinder, 4 stroke engine setup having 80 mm bore and 110 mm stroke with rated power 3.7 kW at 1500 rpm and at 50% load. Fuels with different blends are used that are neat Diesel (E0), 5% blend of ethanol (E5), 10% blend of ethanol (E10), 15% blend of ethanol (E15) and 20% blend of ethanol (E20). Results represented that BSFC decreases as CR increases for all fuel blends. Additionally, BSFC increases as amount of ethanol in the blend increases.

Raheman et al. [28] conducted a study on the effect of engine load, injection timing and different blends of biodiesel obtained from mahua oil by using a single cylinder, 4 stroke engine setup having 76.2 mm bore and 111.1 mm stroke with maximum power 9 kW at CR values 18, 19 and 20. The study showed that BSFC decreases with increasing CR, engine load. Decrease trend is observed for all injection timing and fuel blend values.

Vasudeva et al. [29] used esters of crude rice bran oil and neat Diesel fuel and reported that BSFC decreases as CR increases at 60% and 100% engine loads. Additionally, Hirkude et al. [30] used waste fried oil methyl ester blends and neat Diesel fuel and assessed the effect of CR on BSFC. Results represented that BSFC decreases as CR increases.

Literature survey also revealed that fuel consumption is lower in higher engine loads. Besides, it is recognized that fuel consumption increases when the amount of the neat Diesel fuel decreased in the fuel blend [27 - 30].

2.2.2.2. Compression Ratio Effect on Brake Thermal Efficiency

Maximum engine efficiency is aimed in order to increase the cost efficiency of both gasoline and Diesel engine systems. Diesel engines are known to have higher thermal efficiency compared to gasoline engines.

BTE values are calculated in the present work with the knowledge of BSFC data presented in Section 2.2.2 and fuels' lower calorific values involved in the associated published studies [27-30]. As a result, Figure 2.9 is obtained.

In Figure 2.9, it is observed that BTE increases with increasing CR as expected even if different fuel type, engine load, fuel injection pressure and injection timing etc. are used. Besides, it is acknowledged that the LCV value of the Diesel fuels is higher than the biodiesel fuels which results in higher BTE [27, 31].

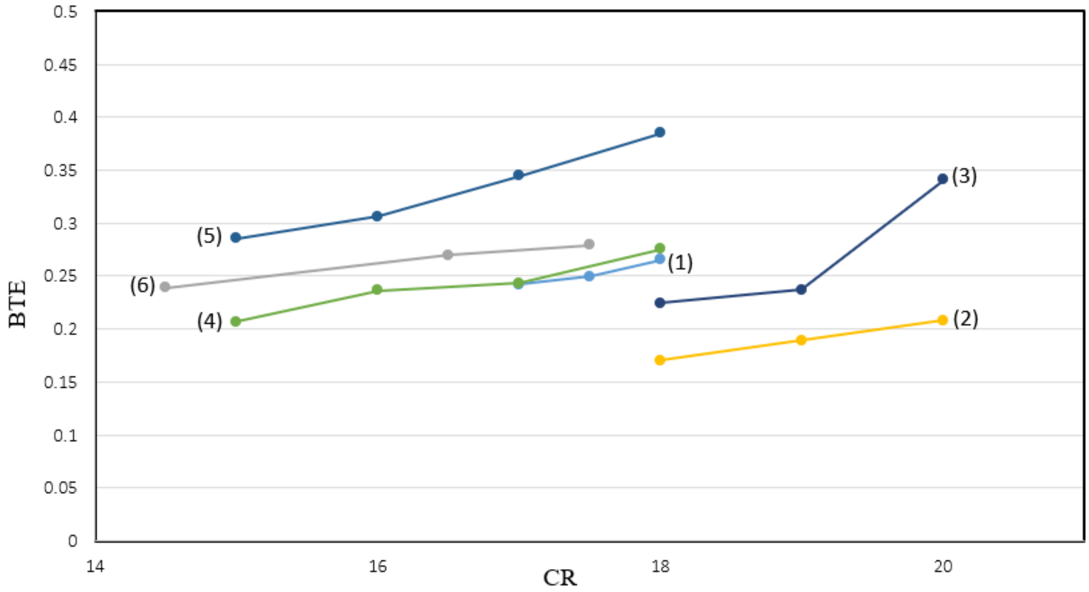

Legends of Figure 2.9.	(1)	(2)	(3)	(4)	(5)	(6)
Engine power (kW)	3.7	9	9	3.75	3.75	3.78
# of cylinder	1	1	1	1	1	1
# of stroke	4	4	4	4	4	4
Bore (mm)	80	76.2	76.2	87.5	87.5	80
Stroke (mm)	110	111.1	111.1	110	110	110
Speed (rpm)	1500	1500	1500	1500	1500	1500
IT (°)	-	35-45 bTI	35-45 bTDC	23 bTDC	23 bTDC	27 bTDC
IP (bar)	-	-	-	195	195	190
Fuel	Diesel	Diesel	Diesel	Diesel	Diesel	Diesel
Load (%)	50	50	100	60	100	100
Reference	[27]	[28]	[28]	[29]	[29]	[30]

Figure 2.9. BTE variation with compression ratio

2.2.2.3. Compression Ratio Effect on Emission

NO_x Emission

As it is mentioned in Section 1.1.1, thermal NO_x formation highly depends on the temperature reached in the cylinder during engine operation. Since Diesel engines have higher in-cylinder temperatures NO_x emission is higher. Increase in CR causes increase in the temperature reached and results in increase in NO_x emission amount. Additionally, when the engine speed is lower, it means longer time is available for the NO_x formation reactions therefore NO_x emission increases [25].

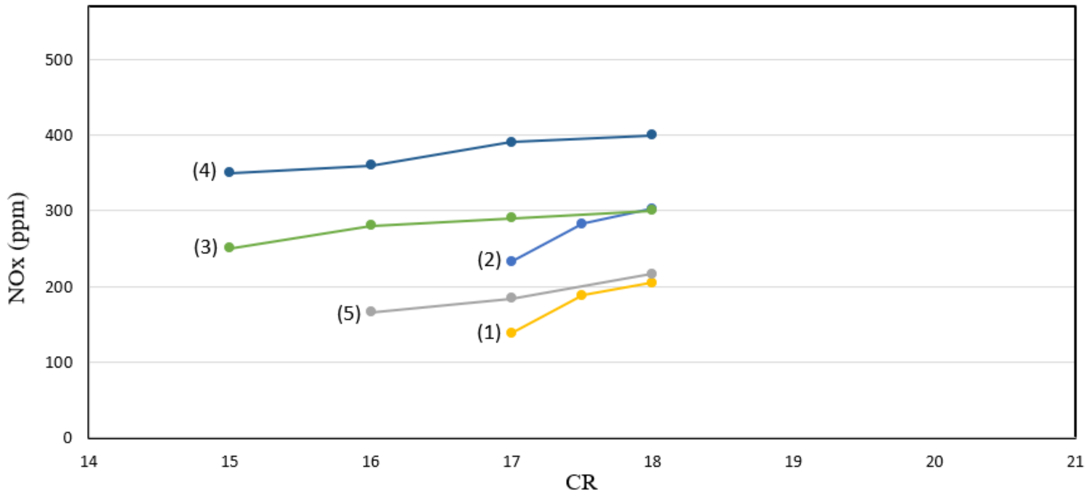

Legends of Figure 2.10.	(1)	(2)	(3)	(4)	(5)
Engine power (kW)	3.7	3.7	3.75	3.75	3.5
# of cylinder	1	1	1	1	1
# of stroke	4	4	4	4	4
Bore (mm)	80	80	87.5	87.5	87.5
Stroke (mm)	110	110	110	110	110
Speed (rpm)	1500	1500	1500	1500	1500
IT (°)	-	-	23 bTDC	23 bTDC	23 bTDC
IP (bar)	-	-	195	195	210
Fuel	Ethanol E20	Diesel	Diesel	Diesel	Jatropha methyl ester B100
Load (%)	50	50	60	100	100
Reference	[27]	[27]	[29]	[29]	[31]

Figure 2.10. NO_x emission variation with compression ratio

Results from various published work are collected and plotted in Figure 2.10 in order to observe the effect of CR on NO_x emission for Diesel engines. All the curves have a increase trend with increasing compression ratio even if different fuel type, engine load, fuel injection pressure or injection timing are used [27, 29, 31].

Kurre et al. [27] investigated the effect of CR values 17, 17.5 and 18 on NO_x emission at 50% part load. Fuels with different blends are used that are neat Diesel (E0), 5% blend of ethanol (E5), 10% blend of ethanol (E10), 15% blend of ethanol (E15) and 20% blend of ethanol (E20). Results represented that NO_x emission increases as CR increases for all fuel blends and engine loads.

Vasudeva et al. [29] used esters of crude rice bran oil and neat Diesel fuel. It was reported that NO_x emission increases as CR increases at 60% and 100% engine loads. Additionally, Jindal et al. [31] used jatropha methyl ester to examine the effect of CR on NO_x emission. As other two studies, it was also reported that NO_x emission increase with increasing CR.

Studies also revealed that neat Diesel fuel causes more NO_x emission compared to other fuels such as ethanol and jatropha methyl ester blends [27, 31].(See Figure 2.10) Furthermore, Vasudeva et al. showed that NO_x emission increases when engine load increases [29].

CO_2 Emission

CO_2 emission is directly related to fuel consumed during the operation of the engine [25]. Figure 2.8 shows that fuel consumption decreases with while CR increases. Lower fuel consumption results in lower CO_2 emission. Therefore, it is observed that CO_2 emission decreases with increasing CR while NO_x emission increases.

2.2.3. Effect of the SCR Unit on Diesel Engine Performance

Engine exhaust gas is exposed to a resistance along the aftertreatment system until it reaches the atmosphere. This resistance is called "backpressure" in aftertreatment applications [48]. SCR deNO_x units form a part in total backpressure along with other aftertreatment equipment. (DOC, DPF, muffler etc.)

Engine needs to work harder to be able to pump the exhaust gases out of the cylinder against the high resistance. Hield et al. [49] reported the PV diagram in Figure 2.11 in which arrows represent the variations with increasing backpressure. A logarithmic scale is used for the pressure axis to observe the variations more clearly. In the figure, increase in the area of pumping loop can be observed for increasing backpressure. It means the work done by the piston increases to overcome the backpressure and vent the gas out of the cylinder. When backpressure increases, more fuel consumption is required to overcome the increased pumping work while maintaining the same brake power. Hield et al. [49] obtained Figure 2.12 that indicates the BSFC change with the increasing backpressure. Furthermore, increase in BSFC yields increase in CO_2 emissions as mentioned in Section 2.2.2.3.

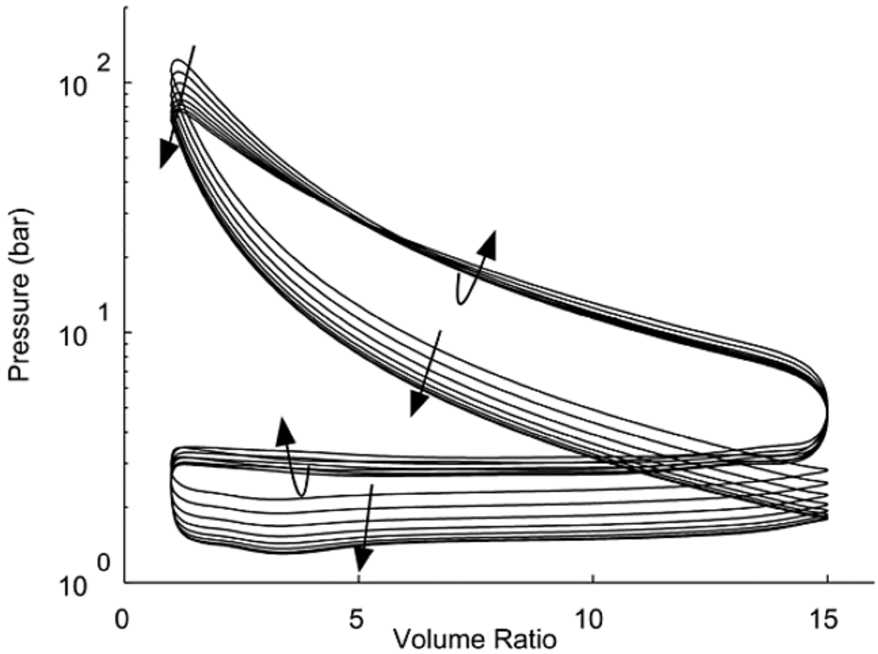

Figure 2.11. Actual PV diagram of a Diesel engine. Arrow directions represent the change with increasing backpressure [49]

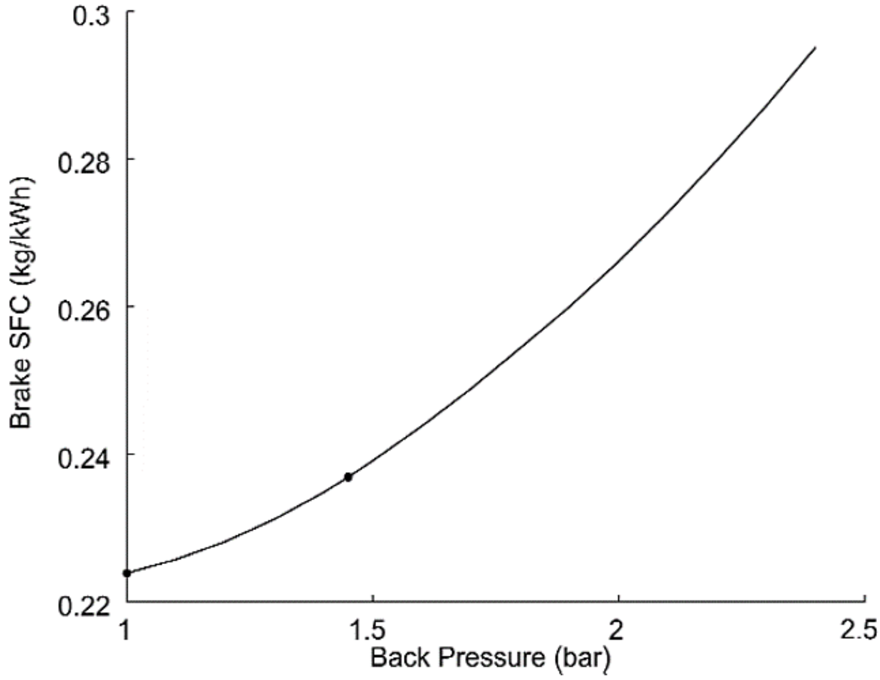

Figure 2.12. BSFC change with increasing backpressure [49]

In addition to increase in pumping work, another significant impact of the backpressure is on the amount of post-combustion gases which are trapped in the engine cylinder due to high pressure resistance at engine exit. Residual gases in the cylinder have a negative impact on the intake of fresh fluid inside the cylinders. Cong et al. [50] defined residual gas fraction (RGF) term and investigated how it is influenced by backpressure in a conventional Diesel engine at 1500 and 2500 rpm engine speeds and 8 mg and 16 mg injected fuel amount in one cycle are examined in the work. The study revealed that RGF in the engine cylinder increases with increasing backpressure.

Burnete et al. [51] conducted an experimental study to observe the backpressure effects on the engine performance. In this study, a flap is located at the different locations along the exhaust system which provides the capability of observing which location of flap gives the best results. The study showed that location of the flap influences the maximum engine power and torque obtained. Maximum engine power decreases when flap is located at a further location.

CHAPTER 3

METHODOLOGY

3.1. SCR Unit Modeling

SCR deNO$_x$ unit modeling is performed by using COMSOL Multiphysics® Software. The model is used to compute pressure drops at different engine exhaust mass flow rates while keeping NO conversion at 98%.

Firstly, an SCR unit geometry with 600 cpsi cell density is built. While building the geometry, symmetrical form of the unit due to its cylindrical form and the repetition feature of the channels are used to simplify the model. Then the pressure drops at different engine exhaust mass flow rates are computed. Before performing pressure drop calculations, an experimental data [32] is used for model verification.

Secondly, NO conversion is computed in the model and verified by considering whether the values match with the ones in literature [40, 41, 43, 44].

3.1.1. Geometry of the SCR Unit

As it is mentioned in 2.1.1, honeycomb structure of the monolith reactor used in SCR deNO_x units is formed by repetition of reactive channels washcoated by a catalyst such as precious metals (Pt etc.), metal oxides (V_2O_5 - TiO_2 etc.) and metal-exchanged zeolites (Cu-zeolite, Fe-zeolite etc.). Geometry of the monolith reactor has an important role on pressure drop between the inlet and the outlet. Cell density of the monolith is a significant parameter for the pressure drop calculations and defined as [34]

$$N = \frac{1}{a^2} \qquad (15)$$

Where N is the cell density of the monolith reactor (cell per square mm) and a is the cell spacing of a single reactive channel (mm). In literature, "cpsi" expression is commonly used which stands for "cell per square inch".

Hydraulic diameter of a single reactive channel is defined as [34]

$$D_h = a - t \qquad (16)$$

Where t is the thickness of the supporting wall (mm). Figure 3.1 indicates cell spacing (a), wall thickness (t), hydraulic diameter (D_h) and the washcoated area of a single reactive channel in a SCR deNO_x unit.

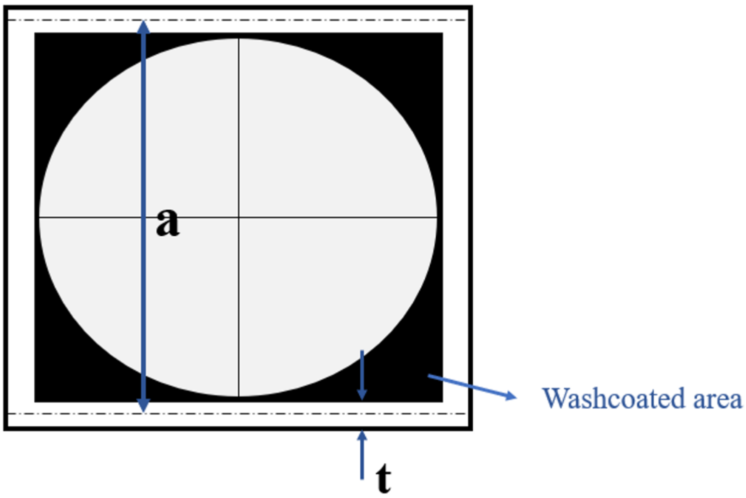

Figure 3.1. A single reactive channel cell spacing (a), wall thickness (t) and washcoated area (area shaded with black)

A high cell density provides a large surface area for catalyst surface activities however causes a higher pressure drop between the ends of the monolith reactor. Table 3.1 indicates the result of cell spacing (a) and hydraulic diameter (D_h) calculations performed in the present work. Published cell density (N) and thickness(t) data for commercial automotive ceramic substrates [33] are substituted into equations (15) and (16) to obtain the related cell spacing and hydraulic diameter values.

In the present study, 600 cpsi cell density and the related hydraulic diameter (0.935 mm) is used since the mass flow rate data used in pressure drop calculations belonged to an off-road Stage V engine that requires a SCR deNO$_x$ unit with high cell density to achieve the emission control target stated in regulations. 300-400 cpsi cell densities are common in the market therefore 600 cpsi cell density is adopted in the present work to observe one step further. Besides, using 600 cpsi density brings the benefit that the experimental data from Amirnordin et al. [14] could be used to verify the SCR model.

Table 3.1. Cell spacing and hydraulic diameter values calculated from commercial ceramic substrates data used in automotive SCR deNOx units

Williams et al [33]		Computed in present work		
Cell density N (cpsi)	**Thickness t (mm)**	**Cell Spacing a (inch)**	**Cell Spacing a (mm)**	**Hydraulic Diameter D_h (mm)**
25	0.889	0.200	5.080	4.191
50	0.635	0.141	3.592	2.957
100	0.381	0.100	2.540	2.159
200	0.267	0.071	1.796	1.529
300	0.203	0.058	1.466	1.263
400	0.102	0.050	1.270	1.168
600	0.102	0.041	1.037	0.935
900	0.051	0.033	0.847	0.796

1/8 of the complete monolith is used for calculations to benefit from the symmetry feature. (See Figure 3.2) Similarly, in order to obtain simplicity during model calculations, monolith blocks are introduced to the model which in fact consist of hundreds of reactive channels. (See Figure 3.3) Therefore, not each reactive channel can be observed in the model geometry. To be able to reflect the effect of the hundreds of reactive channels, monolith blocks are assumed porous media having permeability value. Permeability term is used for porous medium to represent the ability of transmitting the flow. Details of the permeability calculation for the monolith blocks and its relation with pressure drop will be clarified in following chapters.

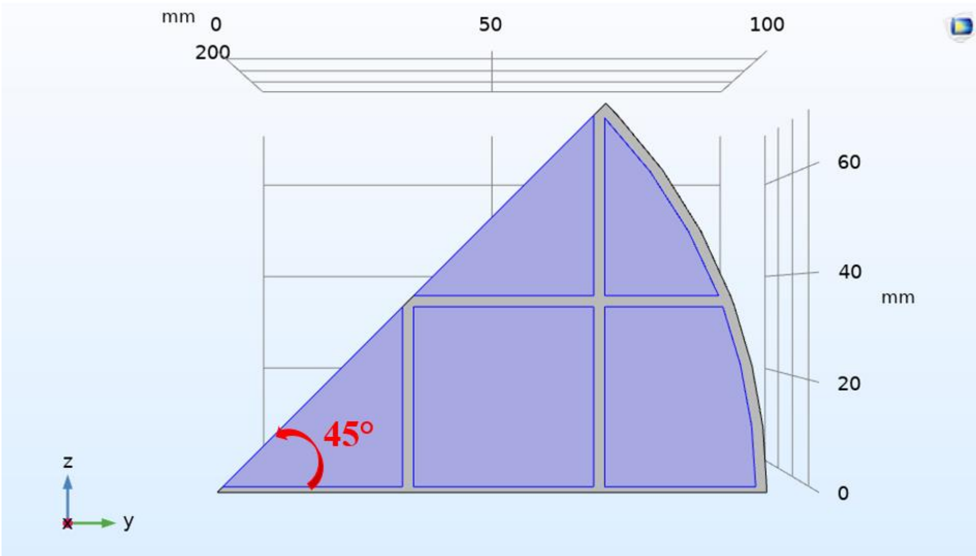

Figure 3.2. 1/8 of the complete monolith reactor (20 cm diameter)

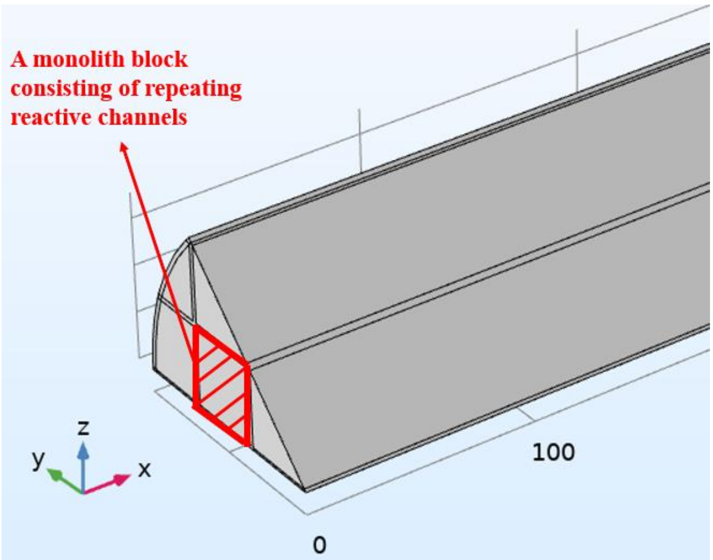

Figure 3.3. A monolith block consisting of hundreds of reactive channels

Primarily, a geometry with 20 cm diameter is used as the minimum SCR deNO$_x$ unit diameter while performing calculations. As it is mentioned in Section 2.2.1, 96-140 kW engines are used with the 20 cm diameter-catalytic converter units. Since the reference engine used in the present work is 202 kW, 20 cm diameter is used as the minimum diameter. After obtaining the pressure drop results for the 20 cm diameter-monolith, diameter is increased up to 25 cm with 1 cm increment with the aim of reducing the monolith length and in turn pressure drops.

3.1.2. Mass Transport and Heat Transfer in the SCR Unit

Mass transport and heat transfer parts of the model are obtained from 3D monolith reactor model in COMSOL Multiphysics® applications [32].

Mass Transport

The system is assumed steady state therefore convection-diffusion equation is used in the steady state form. The equation is defined as

$$\underbrace{\nabla.(-D_i \nabla c_i)}_{\text{Diffusion}} + \underbrace{\boldsymbol{u}.\nabla c_i}_{\text{Convection term}} = \overbrace{R_i}^{\text{Reaction term}} \qquad (17)$$

where D_i is the diffusion coefficient (m^2/s), c_i is the concentration of the species (mol/m^3), **u** is the velocity vector (m/s) and R_i is the rate expression of the species ($mol/m^3.s$).

In the present work, diffusive and convective mass transport are allowed in x direction only (channel direction). **u** in the convection term is common with the **u** represented in Darcy Law. Species transport properties are employed to the model in CHEMKIN data format.

Heat Transfer

Since the system is assumed steady state, temperature equation describing heat transfer in SCR model is defined as

$$\rho\, c_p\, \boldsymbol{u} \,.\nabla \mathrm{T} = \nabla.\left(k_{eq} \nabla \mathrm{T}\right) + Q \qquad (18)$$

where T is the temperature (K), ρ is the density of the fluid (kg/m^3), c_p is the heat capacity of the fluid (J/m^3.K), k_{eq} is the equivalent thermal conductivity (W/m.K) and Q is the heat source which is due to exothermic reactions occurred in SCR unit (W/m^3).

Working fluid is defined as nitrogen since its concentration is significantly high compared to other compounds in the SCR inlet gas mixture. Required properties [32].of the reactor structure are manually entered to the model.

Equivalent thermal conductivity is defined as

$$k_{eq} = (1 - \Theta_L)k_p + \Theta_L k_L \qquad (19)$$

where Θ_L is the porosity of the medium which is 0.75, k_p is the conductivity of the supporting walls (W/m.K), and k_L is the conductivity of the fluid (W/m.K). k_p is defined as 35 (W/m.K) and k_L is defined as 0.13 (W/m.K) in x direction and 0.25 (W/m.K) in y and z directions [32].

Only conduction applies to supporting walls and defined as

$$0 = \nabla.\left(k_p \nabla \mathrm{T}\right) \qquad (20)$$

Following convective heat flux equation is used for the SCR deNOx unit outer walls

$$\mathrm{q}'' = \bar{h}\,.(\mathrm{T} - T_{amb}) \qquad (21)$$

where q is the convective heat flux (W/m^2), $\bar{h}$ is the average heat transfer coefficient (W/m^2.K) which is adopted as 10 (W/m^2.K) [32] and T_{amb} is the ambient temperature (K).

Inlet temperature is equal to each exhaust cases' own temperature. In the model, temperature variation along the channel direction would impact the chemical kinetics, fluid density and fluid dynamic viscosity. However, it is recognized that the model could be assumed isothermal since the temperature change along the channel is less than 1%. The reason is that concentrations of NO and NH_3 compounds, which form

SCR reactions, are very low in the inlet gas mixture therefore the temperature effect is negligible.

3.1.3. Controlling Regime in the SCR Unit

Vanadia-titania washcoated monolith is used as the catalyst element for the model in the present study. Three main controlling regimes can be observed in this element: external mass transfer, internal mass transfer and reaction. Additionally, if a zeolite washcoat is used, intracrystalline mass transfer should be considered as well as other regimes [45].

Joshi et al. and Metkar et al. [45, 47] used a resistance-in-series method to observe the effect of each regime on the SCR system. The same approach is adopted in present work to observe the controlling regimes in the SCR unit. Resistances associated to external mass transfer, internal mass transfer and reaction are calculated as described below.

External mass transfer resistance ($R_{external}$):

$$R_{external} = \frac{4d_{\Omega 1}}{Sh_e(z)D_i} \quad (22)$$

where $Sh_e(z)$ is the Sherwood number (1). NO diffusivity is calculated in COMSOL as D_i=2.925 x 10^{-5} at SCR conditions. Since the entrance effects are neglected in this study, constant value of $Sh_e = 4.36$ is used which is for circular channels [47]. $d_{\Omega 1}$ is the effective transverse diffusion length and defined as

$$d_{\Omega 1} = \frac{A_{\Omega 1}}{P_{\Omega 1}} \quad (23)$$

where $A_{\Omega 1}$ is the reactive channel cross-sectional area (m^2) and $P_{\Omega 1}$ is the washcoat-fluid interface perimeter (m). (See Figure 3.4)

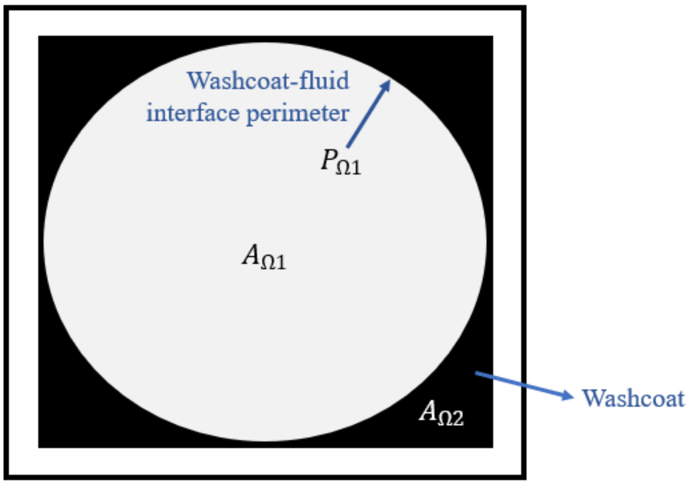

Figure 3.4. Washcoat-fluid interface perimeter ($P_{\Omega 1}$), reactive channel cross-sectional area ($A_{\Omega 1}$) and washcoat cross-sectional area ($A_{\Omega 2}$)

Internal mass transfer resistance ($R_{internal}$):

$$R_{internal} = \frac{d_{\Omega 2}}{Sh_i D_e} \qquad (24)$$

where D_e is the effective diffusivity in Vanadia-titania washcoat (m^2/s) and taken as 3.5 x 10^{-6} [36]. Sh_i is the internal Sherwood number. Balakotaiah [56] came up with a general expression for the internal Sherwood number as below

$$Sh_i = Sh_{i,o} + \frac{\Lambda \Phi^2}{1 + \Lambda \Phi} \qquad (25)$$

$Sh_{i,o}$ and the constant Λ depend on the washcoat geometry. It is assumed that the thickness of the washcoat is constant along the channel and the inner line of the washcoat is circular. Therefore, $Sh_{i,o}$ and Λ are taken as 3 and 0.32 respectively [45, 47]. Thiele modulus here (Φ) is as follows

$$\Phi = d_{\Omega 2} \sqrt{\frac{k}{D_e}} \qquad (26)$$

$d_{\Omega 2}$ is the effective transverse diffusion length in washcoat and defined as

$$d_{\Omega 2} = \frac{A_{\Omega 2}}{P_{\Omega 1}} \qquad (27)$$

where $A_{\Omega 2}$ is the washcoat cross-sectional area (m^2). (See Figure 3.4) k is the rate constant defined by Arrhenius Law.

$$k = A \exp\left(\frac{-E_A}{RT}\right) \qquad (28)$$

where A is the frequency factor (1/s), E_A is the activation energy (J/mol) and R is the universal gas constant 8.314 J/(mol.K). Frequency factor and activation energy are obtained from published works [45, 46].

Reaction resistance:

$$R_{reaction} = \frac{1}{k d_{\Omega 2}} \qquad (29)$$

Table 3.2 shows each resistance value obtained from above resistance expressions.

Table 3.2. Resistances associated to external mass transfer, internal mass transfer and reaction

	Calculated resistance values
$\boldsymbol{R_{external}}$	7.45
$\boldsymbol{R_{internal}}$	2.95
$\boldsymbol{R_{reaction}}$	0.67
$\boldsymbol{R_{total}}$	11.1

The total resistance is the sum of three resistance expressions that are described above.

$$R_{total} = R_{external} + R_{internal} + R_{reaction} \qquad (30)$$

A practical method is raised to decide the controlling regime in the SCR system. In the method, it is suggested that if one of three resistances achieve 90% of the total resistance, it is the controlling regime [47]. According to this approach, reaction regime does not control the system. Besides, external mass transfer has the highest impact on the system. Hence, the effect of various inlet mass flow rates and monolith geometry shapes on SCR performance is observed in the current study since those parameters affect external mass transfer.

3.1.4. Pressure Drop in the SCR Unit

Reynolds number (Re) is calculated at maximum SCR inlet mass flow rate using working fluid's density and dynamic viscosity at 700 K. Re is calculated as 616 which is less than 2300. Therefore, the flow is taken as laminar and also assumed fully developed. In present work, continuity equation and Darcy Law are used to define the flow and pressure drop in the channel.

Continuity Equation:

$$\nabla.(\rho\mathbf{u}) = 0 \qquad (31)$$

Darcy Law:

$$\boldsymbol{u} = -\frac{\kappa}{\mu}\nabla P \qquad (32)$$

Where $\boldsymbol{\kappa}$ is the permeability of the monolith block (m^2), μ is the dynamic viscosity of the engine exhaust gas at SCR inlet (Pa.s) and P is the pressure (Pa).

Permeability can be calculated from experimental results as follows;

$$\kappa = \frac{u\,\mu\,L}{\Delta P} \qquad (33)$$

Permeability calculation is performed for the 600 cpsi monolith and the pressure drop values in the model are verified by using this permeability against a published experimental data [32].

Other two important model parameters are normal inlet velocity and outlet pressure. Relative outlet pressure at SCR exit is assumed zero. In fact, it is not zero since the

SCR unit does not open to atmosphere directly. Since the main purpose in the present work is to obtain the pressure drop along the channel, the relative outlet pressure is assumed zero. Furthermore, it should be noted that all pressure values involved in this study represent relative pressure.

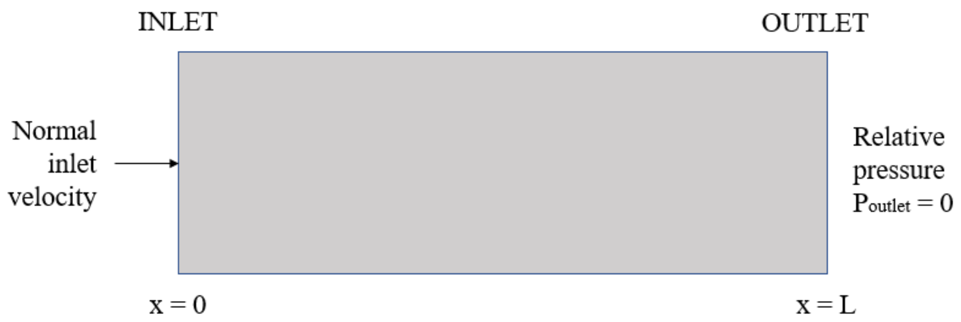

Figure 3.5. SCR $deNO_x$ unit inlet and outlet

Normal inlet velocity is calculated from real engine exhaust mass flow rate data [10]. Entire exhaust system is assumed steady state therefore mass flow rate remains constant from the engine exit to the SCR inlet even if the engine exhaust gas enters the other aftertreatment equipment such as DPF or DOC before entering SCR $deNO_x$ unit.

Normal inlet velocity is computed as

$$u = \frac{\dot{m}}{\rho A} \qquad (34)$$

where $\dot{m}$ is the engine exhaust mass flow rate (kg/s) and A is the open frontal area (m^2) of the SCR $deNO_x$ unit.

Open frontal area of the SCR unit is constant along the channel and calculated by using the number of reactive channels and their frontal area. The frontal area of each reactive channel is obtained by using their hydraulic diameter calculated in Section

3.1.1. Hydraulic diameter value of 600 cpsi-geometry is used for calculations. (See Table 3.1)

Engine exhaust gas density at SCR inlet depends on the temperature and pressure. Engine exhaust temperature is available in the published data [10]. However, the pressure is iterated by giving an initial value and then replaced with the result obtained from pressure calculations.

3.1.4.1. Mesh Independence Analysis

Mesh independence analysis is performed for the same model that is used in the verification process. Pressure drop along the channel is obtained at three different mesh sizes. Number of meshes and obtained pressure drops at each mesh size are stated in Table 3.3. Moreover, it is known that the experimental result for this particular case is 417 Pa [14]. The variation between experimental and model results is less than 0.2%.

Table 3.3. Pressure drop values at three different mesh sizes

# of elements	**Pressure Drop (Pa)**
260600	416.2
130300	416.2
26060	416.2

The mesh independence analysis showed that increasing number of elements does not affect the solution obtained. Therefore 26060 elements, which is the default value defined by COMSOL, is used for the further calculations regarding simplicity.

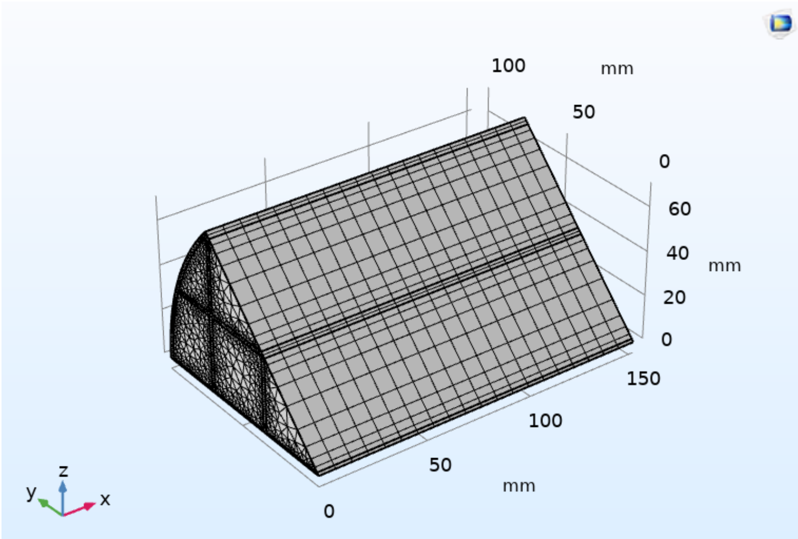

Figure 3.6. The model geometry with 26060 mesh elements

3.1.5. NO_x Conversion in the SCR Unit

As it is mentioned in 1.1.1, the main concern in the NO_x emission issue is the emission of NO since it forms 95% of entire NO_x emissions [8].

NO conversion is used to represent the performance of the SCR deNO_x unit. NO conversion along an SCR unit is computed as

$$NO\ Conversion\ (\%) = \left(\frac{c_{NOi} - c_{NOe}}{c_{NOi}}\right).100 \qquad (35)$$

where c_{NOi} and c_{NOe} are NO concentrations at SCR unit inlet and outlet respectively (mol/m^3).

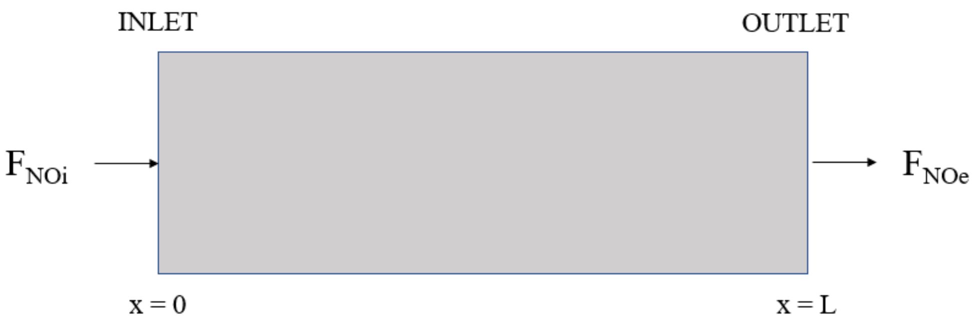

Figure 3.7. SCR deNO$_x$ unit inlet and outlet molar flow

General molar balance around the SCR unit is given below

$$F_{NOi} - F_{NO} + \int r'_{NO} dW = \frac{dN_{NO}}{dt} \qquad (36)$$

where F_{NOi} is the molar inlet flow of NO (mol/s), F_{NO} is the instant molar flow of NO (mol/s), r'_{NO} is the reaction rate in terms of catalyst mass (mol/kg.s), W is the catalyst mass (kg catalyst), N_{NO} is the mol of NO (mol) and t is the time (s).

Since the system is assumed to operate at steady state, equation (36) is simplified as

$$F_{NOi} - F_{NO} + \int r'_{NO} dW_{cat} = 0 \qquad (37)$$

NO conversion along the monolith reactor is defined as

$$X_{NO} = \frac{F_{NOi} - F_{NOe}}{F_{NOi}} \qquad (38)$$

where

$$F_{NOj} = \upsilon_0 \, c_{NOj} \qquad (39)$$

$$\upsilon_0 = \rho \, \dot{m} \qquad (40)$$

X_{NO} is NO conversion along the monoltih, F_{NOj} is the molar flow (mol/s), υ_0 is the volumetric flow rate (m^3/s) and c_{NOj} is the NO concentration (mol/m^3).

Equation (38) can also be written as

$$F_{NOi} - F_{NOe} = X_{NO}\, F_{NOi} \qquad (41)$$

Doing the arrangements for inlet and outlet molar flow to obtain X_{NO}

$$X_{NO} = \frac{1}{F_{NOi}}(-r'_{NO})(W_{cat}) \qquad (42)$$

Substituting (39) and (40) into (42)

$$X_{NO} = \frac{1}{\rho\, \dot{m}\, c_{NOi}}(-r'_{NO})(W_{cat}) \qquad (43)$$

As it is seen in equation (43), NO conversion along the monolith depends on reaction rate, catalyst mass, inlet NO concentration, density and mass flow rate of engine exhaust gas at SCR inlet. When the cell density of the monolith increases, the mass of the catalyst increases and it leads to increase in NO conversion. If the SCR inlet temperature increases, reaction rate increases and the gas density decreases. Therefore, NO conversion along the channel increases. Additionally, conversion decreases as mass flow rate increases.

If (43) is rewritten by considering the catalyst volume this time instead of catalyst mass;

$$X_{NO} = \frac{1}{\upsilon_0\, c_{NOi}}(-r_{NO})(V_{cat}) \qquad (44)$$

where r_{NO} is the reaction rate in terms of catalyst volume (mol/m^3.s) and V_{cat} is the catalyst volume (m^3).

Regarding catalyst volume, space time and space velocity are significant parameters for SCR $deNO_x$ unit sizing. Space time is the period spent by engine exhaust gas in the SCR $deNO_x$ unit whereby the space velocity is 1/(space time).

Space velocity and space time are defined as

$$SV = \frac{\upsilon_0}{V_{cat}} = \frac{1}{\tau} \qquad (45)$$

SV is space velocity (s^{-1}) and τ is the space time (s).

Re-writing (44) by using space time (τ) and space velocity (SV)

$$X_{NO} = \frac{1}{c_{NOi}}(-r_{NO})(\tau) = X_{NO} = \frac{1}{SV\ c_{NOi}}(-r_{NO}) \qquad (46)$$

To be able to understand the effect of the inlet gas velocity on conversion, the following equations are used.

υ_0 and V_{cat} can be written as

$$\upsilon_0 = u\,A \qquad (47)$$

$$V_{cat} = L\,A \qquad (48)$$

where L is the length of the monolith(m).

Using (47) and (48), (45) is simplified to

$$SV = \frac{u}{L} \qquad (49)$$

Substituting (49) into (46)

$$X_{NO} = \frac{L}{u\ c_{NOi}}(-r_{NO}) \qquad (50)$$

Equation (50) reveals that NO conversion along the SCR deNO_x unit increases when the unit length increases. However, Darcy Law states that pressure drop increases when the unit length increases. The pressure drop increase causes more resistance to engine exhaust gas to reach atmosphere.

In the present work, 98% NO conversion is aimed to achieve the NO_x emission targets stated in the Stage V regulation for the SCANIA 9 L off-road Diesel engine at different engine exhaust mass flow rates. While keeping the NO conversion at 98%, SCR deNO_x units with different diameter and length are assessed in terms of pressure drop. In addition, the impact of the inlet gas temperature on NO conversion is observed.

3.1.5.1. Chemical Kinetics

As it is seen in equations (43, 50), NO conversion is directly related to the reaction rate. In the present work, equation (6), which is called "standard SCR reaction", is employed to describe the NO reduction chemistry. Equation (6) is an equimolar reaction in terms of NO and NH_3.

However, NH_3 is oxidized simultaneously and it causes a reduction in NH_3 amount that is supposed to undergo the main NO_x reduction reaction. Therefore, NH_3 oxidation equation (11) is also employed to the system as the side reaction in the present work.

Eley-Rideal mechanism is used to describe the rate of standard SCR reaction. The rate-limiting step of the process is that adsorbed NH_3 reacts with the gas-phase NO. Rate mechanism is described as [36]

$$r_a = k_a c_{NO} \, \frac{\alpha c_{NH3}}{1 + \alpha c_{NH3}} \qquad (51)$$

where

$$k_a = A_a \exp\left(-\frac{E_a}{R_g T}\right) \qquad (52)$$

$$\alpha = A_0 \exp\left(-\frac{E_0}{R_g T}\right) \qquad (53)$$

c_{NO} and c_{NH3} are the concentrations of NO and NH_3 respectively (mol/m^3), r_a is the reaction rate of equation (6) (mol/m^3.s), k_a is the rate constant, A_a is the frequency factor of equation (6) (1/s), A_0 is the frequency factor for correction (1/s), E_a is the activation energy of equation (6) (J/mol), E_0 is the activation energy for corerection (J/mol), R_g is the universal gas constant (J/mol.K).

Rate reaction for equation (11) is described with a first order expression as follows; [36]

$$r_b = k_b c_{NH3} \tag{54}$$

where

$$k_b = A_b \exp\left(-\frac{E_b}{R_g T}\right) \tag{55}$$

r_b is the reaction rate of equation (11) (mol/m^3.s), k_b is the rate constant (1/s), A_b is the frequency factor of equation (11) (1/s), E_b is the activation energy of equation (11) (J/mol). Required activation energy and frequency factor values are taken from a published kinetic information set [36].

3.1.6. Combining Pressure Drop and NO_x Conversion Calculations

As mentioned in Section 2.1.3., to obtain the optimum balance between the conversion efficiency, system cost and fuel consumption, 98+ % SCR is required [40]. Therefore, NO conversion level in the present work are kept at 98% and pressure drop calculations are performed aiming to achieve this conversion efficiency. While calculating pressure drops, data of DC09 078A type SCANIA industrial engine having 202 kW power output is used.

Since reactions standard SCR reaction and NH_3 oxidation reactions are competing during NO reduction, correct amount of NH_3/NO has to be used to obtain the optimum NO conversion, which is aimed as 98%. To be able to operate the SCR system around 700 K inlet temperatures, NH_3/NO is taken as 2 to be able to obtain 98% NO conversion by using the result of a previous work [30].

In order to calculate the SCR normal inlet velocities, equation (34) is used which needs the information of inlet mass flow rate, gas density and the area. Open frontal area, which can be calculated from the multiplication of the area of a single reactive channel and number of channels involved in a 600 cpsi monolith, is used for the area term in equation (34). SCR unit diameter is taken as 20 cm as a starting point. By increasing the diameter from 20 cm to 25 cm, higher catalyst activity and lower inlet velocities are targeted which in turn provide 98% conversion at an earlier length. 25 cm is used as the highest diameter since it sufficiently decreased the length where 98% conversion obtained and therefore pressure drop decreased significantly.

Inlet gas density depends on the temperature and pressure of the SCR unit inlet. Nitrogen is used for the density calculations since the concentration of nitrogen is significantly high compared to gases in the inlet mixture. Engine exhaust temperatures of the reference engine [10] are used as SCR inlet temperature. Outlet pressure is fixed at atmospheric pressure. In order to calculate the inlet pressure to use in inlet velocity calculations, firstly an inlet velocity is calculated by using equation (34) at inlet temperatures in and atmospheric pressure and then iterated to the correct inlet pressure.

Table 3.4 represents the SCR unit diameter used in the model and associated open frontal areas, number of reactive channels and inlet velocities. Engine exhaust mass flow rate and temperature data at 2100 rpm engine speed are used. Last two rows of the table reveal the length where 98% NO conversion obtained and the pressure drop related to those lengths. Since the inlet velocity decreases with the increasing SCR unit diameter, 98% NO conversion is obtained earlier in the SCR unit having highest diameter.

Table 3.4. Number of monolith channels, conversion and pressure drops at diameters from 20 cm up to 25 cm

D(cm)	20	21	22	23	24	25
Area (m^2)	0.03141	0.03463	0.03801	0.04154	0.04523	0.04908
#of cells in 600 cpsi monolith	29217	32212	35352	38639	42072	45651
Inlet velocity (m/s) (for 2100 rpm engine case)	33.8	30.6	27.9	25.5	23.4	21.6
98% NO Conversion Length (cm)	115	100	80.8	60.1	41.2	28.0
Pressure drop along the monolith (kPa)	29.1	22.9	16.8	11.4	7.12	4.40

3.2. Thermodynamic Analysis of Diesel Engine

Although aftertreatment system equipment (DOC, DPF, SCR, LNT, silencer etc.) in vehicles provide control on emission and noise, they cause pressure drop along the exhaust system starting from the engine exhaust until reaching atmosphere. Thus, pressure of the gas exhausted from the engine has to be at a level that allows exhaust gas to overcome the pressure drop along the exhaust system and reach the atmosphere. In addition, the resistance caused by aftertreatment system may inhibit the ventilation of the gas in the engine cylinder therefore suction volume of the air from the engine intake decreases. This causes decrease in volumetric efficiency of the engine which is defined as the ratio of actual suction volume of air to that of a theoretical suction volume. Hence, the aftertreatment system should be designed in concurrence with the engine not to have engine performance issues. As it is mentioned in Section 2.2.2, compression ratio is a significant parameter in engine thermal efficiency, fuel consumption and NO_x emission considerations. In the present section, the compression ratio effect on the engine efficiency and NO_x emissions is investigated.

3.2.1. Compression Ratio Effect on the Diesel Cycle Efficiency and NO_x Emission

High pressure drop along an SCR unit represents that the SCR unit have higher resistance. The resistance is to be overcome in order to engine exhaust gas to flow to the atmosphere. Otherwise, choking occurs. Compression ratio parameter is selected to enhance the engine efficiency and also to achieve venting of the complete exhaust gas from the exhaust system.

Although designing the engine with higher compression ratio increases both the positive (+W) and negative work (-W), positive work increases more. (See Figure 3.8) Therefore, the efficiency of the engine increases. However, NO_x emission increases with the increasing compression ratio as mentioned in Section 2.2.2.3. (See Figure 2.10. NOx emission variation with compression ratio)

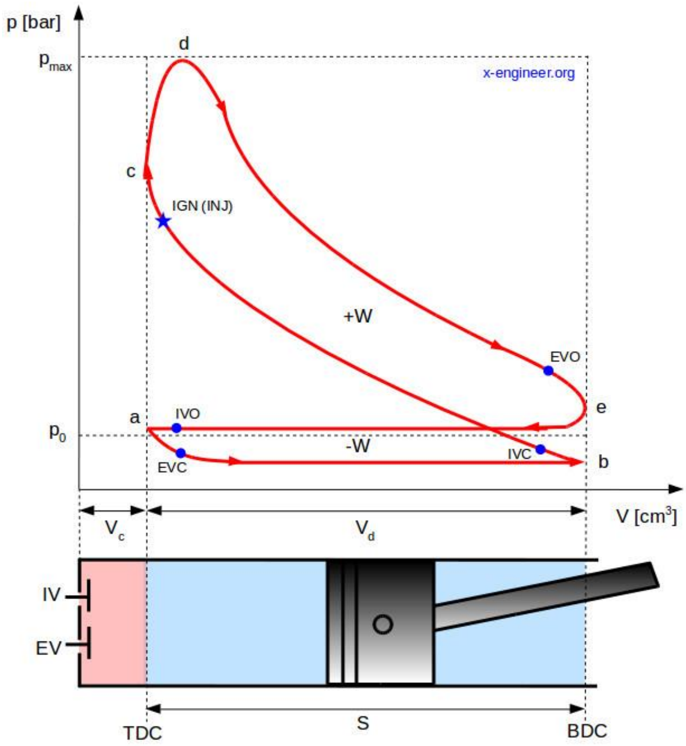

Figure 3.8. An internal combustion engine actual PV diagram [5]

An ideal cycle is examined by aiming a higher engine exhaust pressure to overcome aftertreatment resistance while decreasing the compression ratio to obtain less NO_x emission by being aware of that the engine efficiency will decrease. Since the cycle is <u>ideal</u>, it is acknowledged that the actual efficiencies are much lower. However, the intention here is to observe the effect of the aftertreatment resistance caused by SCR on the thermal efficiency and see whether it has an increasing or decreasing trend to make a comparison.

If the maximum pressure reached in the cylinder and heat addition are assumed constant, higher engine exit pressure can be achieved by decreasing the cylinder stroke. Designing engine with a shorter stroke leads to a lower compression ratio. (See Figure 3.9)

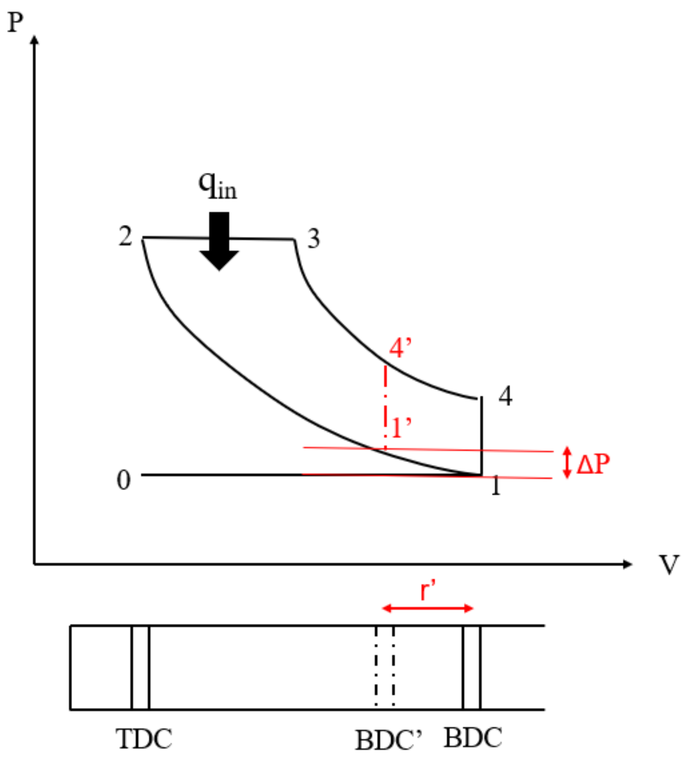

Figure 3.9. Ideal Diesel cycle PV diagram

Since the compression is isentropic in an ideal Diesel cycle, following relations are obtained

$$s_1 = s_{1'} \qquad (56)$$

$$\frac{P_{1'}}{P_1} = r_v' \qquad (57)$$

r_v' is to represent the decrease in the compression ratio.

ΔP in Figure 3.9 indicates the pressure drop caused by SCR unit.

Diesel cycle thermal efficiency is defined as

$$\eta_{th} = 1 - r_v^{1-k} \frac{{r_c}^k - 1}{k(r_c - 1)} \qquad (58)$$

where r_v is the compression ratio, r_c is the cut-off ratio and k is the specific heat ratio.

Compression ratio and cut-off ratio are defined as follows

$$r_v = \frac{V_1}{V_2} \qquad (59)$$

$$r_c = \frac{V_3}{V_2} \qquad (60)$$

Since cut-off ratio is kept constant in this case, only the compression ratio affects the thermal efficiency. It is known that net work of the cycle is the area under 1-2-3-4. Figure 3.9. points out that the area under 1'-2-3-4' is less than the area under 1-2-3-4. Since the thermal efficiency of the cycle is defined as the net work divided by heat added and the heat added is kept constant, thermal efficiency of the cycle decreases.

Although the thermal efficiency of the cycle decreases, cylinder size decreases and provides saving for the system volume and weight. By adding a turbocharger, maximum pressure of the cycle can be increased and the thermal efficiency of the cycle can be increased for the same cylinder size.

CHAPTER 4

RESULTS AND DISCUSSION

Backpressure results obtained for the 600 cpsi SCR deNO$_x$ unit are provided in this chapter. It is recognized that SCR deNO$_x$ units in the market mostly have 300-400 cpsi cell density. However, the results are obtained for 600 cpsi SCR units since the latest emission regulations require higher NO$_x$ conversion performance.

While obtaining results, NO conversion is kept at 98% since it is known that this conversion value gives the best results regarding stringent emission limits, fuel consumption and the opportunity of eliminating EGR [40, 41, 43, 44]. The lengths where 98% NO conversion achieved and associated backpressures are obtained for the SCR deNO$_x$ units with diameter from 20 cm up to 25 cm with 1 cm increment. In addition, the effect of the SCR inlet temperature is examined.

Finally, the results of the ideal cycle analysis by using backpressure results from the model is also involved in this section.

4.1. Model Verification Results

As it is mentioned in Section 3.1.1, monolith blocks are implemented to the model which are assumed porous media having a permeability value. In the present study, permeability of the 600 cpsi monolith was calculated based on a published experimental work. Amirnordin et al. [14] conducted experimental pressure drop analysis for square and hexagonal shaped monoliths in scope of catalytic converters. 600 cpsi cell density was used in the study. Experimental and computed results were compared.

Permeability of 600 cpsi monolith is calculated as 3.33 $x10^{-8}$ m^2 using experimental data by Amirnordin et al. and equation (33). Then, the same conditions with the experiment are substituted to the COMSOL model and the associated backpressure is computed. Experimental conditions used by Amirnordin et al. and used in the present study to verify the pressure drop is stated in Table 4.1.

Table 4.1. Experimental conditions used by Amirnordin et al. and used in the present study to verify the pressure drop

Normal inlet velocity	5 m/s
Dynamic viscosity	1.82 x 10^{-5} Pa.s
Monolith length	0.15 m
Domain material	Air
Inlet temperature	20°C
Permeability calculated using the data above and equation (33)	3.33 x 10^{-8} m^2

416.3 Pa backpressure is obtained from the model by using the conditions in Table 4.1 while the backpressure observed in the experiment was 417 Pa.

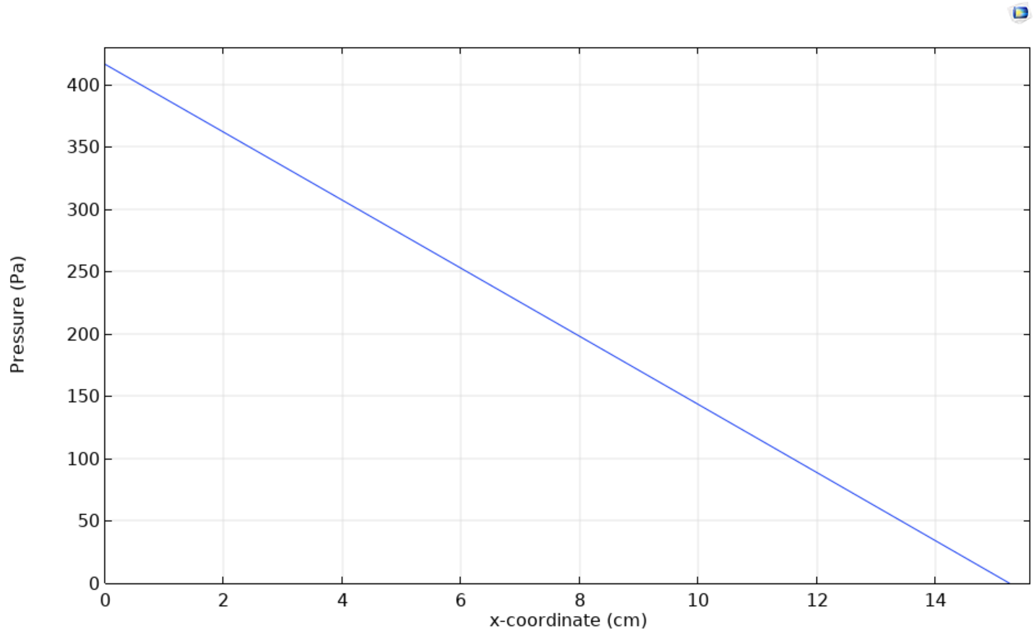

Figure 4.1. Pressure along the monolith channel direction by using the experimental conditions in Ref [14]

0.17% deviation is observed between the experimental data and computed value in the present work. (See Table 4.2) Therefore 3.33 x 10^{-8} m^2 is taken as the permeability value for 600 cpsi monolith geometry for the rest of the calculations.

Table 4.2. Comparison between published experimental data and the pressure drop obtained from the model in present work

Amirnordin et al [14]	Computed in Present Work	
Experimental Pressure drop (Pa)	**Model Pressure drop (Pa)**	**Deviation**
417	416.3	0.17%

4.2. SCR Unit Modeling Results

It is recognized that 96-140 kW engines are used along with 20 cm diameter-catalytic converter units in the market. Since the reference engine of the present work is a 202-kW engine and a higher cell density is used compared to existing products, 20 cm diameter is determined to be used as the minimum diameter sizing. There are 4 cases obtained from the reference engine data [10] that are used for the calculations. Table 4.3 indicates the engine speeds and associated exhaust mass flow rates and temperatures defining those cases.

Table 4.3. Engine speed and associated exhaust mass flow rate and temperature data which define 4 cases used in the present work [10]

	Engine Speed (rpm)	**Engine Exhaust Mass Flow Rate (kg/min)**	**Engine Exhaust Temperature (K)**
Case 1	1200	15	776
Case 2	1500	19	719
Case 3	1800	22	702
Case 4	2100	23	697

As engine speed increases, engine exhaust mass flow rate and SCR unit inlet velocities increase. Figure 4.2. indicates that higher mass flow rate requires more monolith length to achieve 98% NO conversion. Therefore, Case 4 shown in Table 4.3 needs to be considered as the critical case while sizing the SCR unit since all the cases shall be covered regarding the whole operation cycle of the engine and the case with the highest monolith length covers other cases. Likewise, the maximum pressure drop, which in turn creates the highest aftertreatment resistance, is observed at Case 4. (See Figure 4.3)

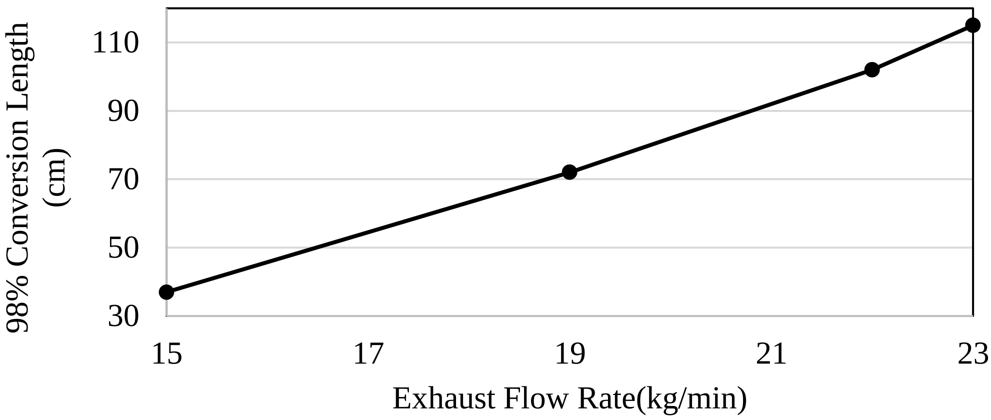

Figure 4.2. Variation of the length where 98% conversion achieved with the increasing engine exhaust mass flow rate

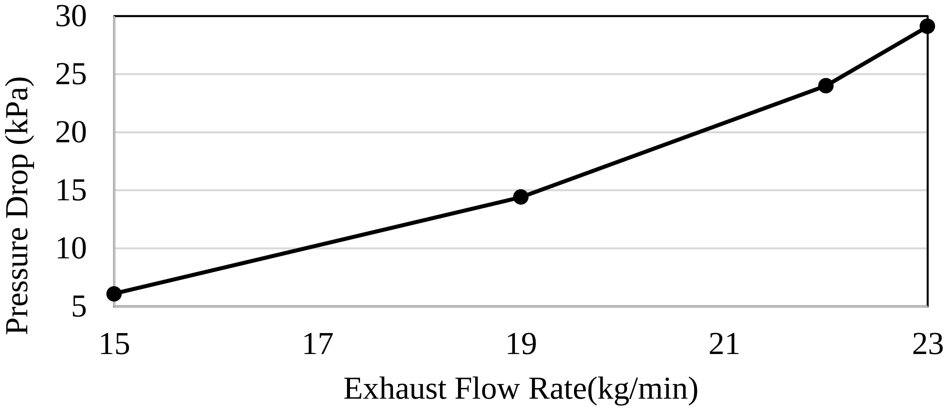

Figure 4.3. Variation of the pressure drop with the increasing engine exhaust mass flow rate

The conversion and pressure drop plots of Case 4 for the 20 cm-diameter SCR $deNO_x$ unit are plotted in Figure 4.4 and Figure 4.5 respectively. Plots obtained for other cases are included in Appendix A.

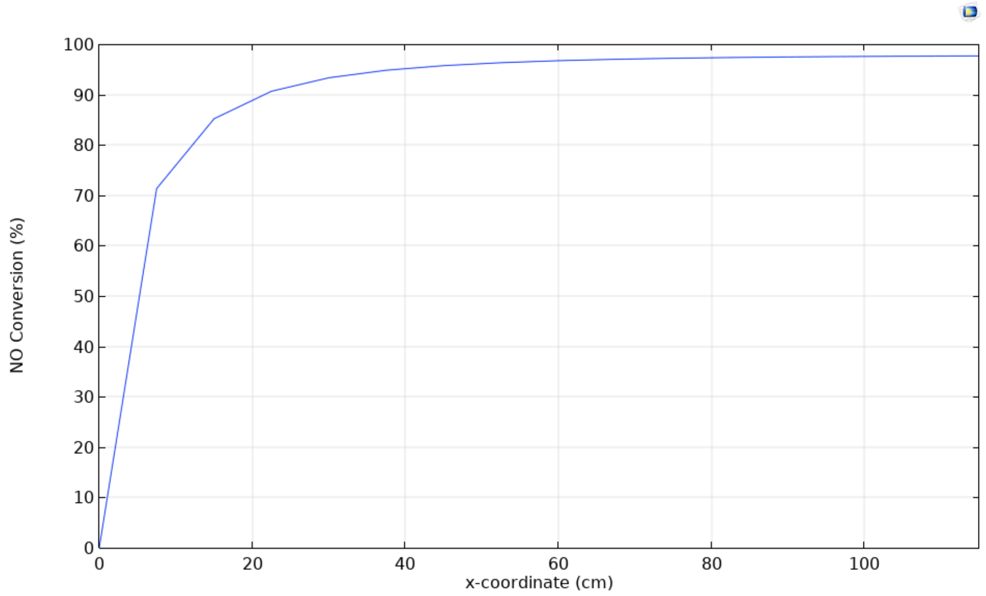

Figure 4.4. NO conversion along the monolith channel direction for Case 4 (SCR unit diameter: 20 cm, NO conversion target at the end of the channel: 98%)

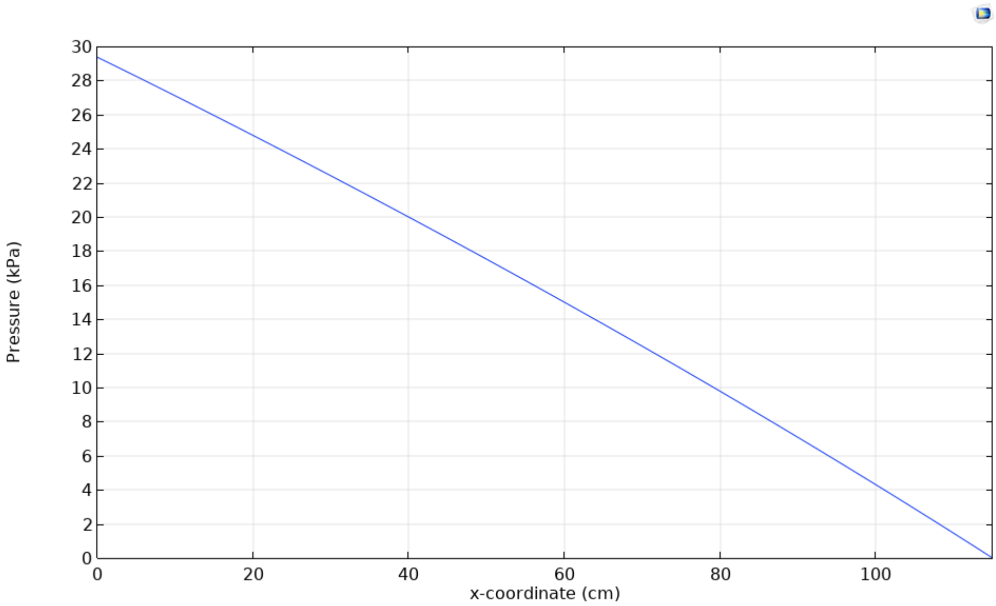

Figure 4.5. Pressure drop along the monolith channel direction for Case 4 (SCR unit diameter: 20 cm, NO conversion target at the end of the channel: 98%)

In the present work, NO conversion is kept at 98% level to achieve latest stringent emission standards, to eliminate EGR and the other concerns noted in Section 2.1.3. However, Figure 4.6. illustrates that 97% conversion can be achieved at 60 cm length.

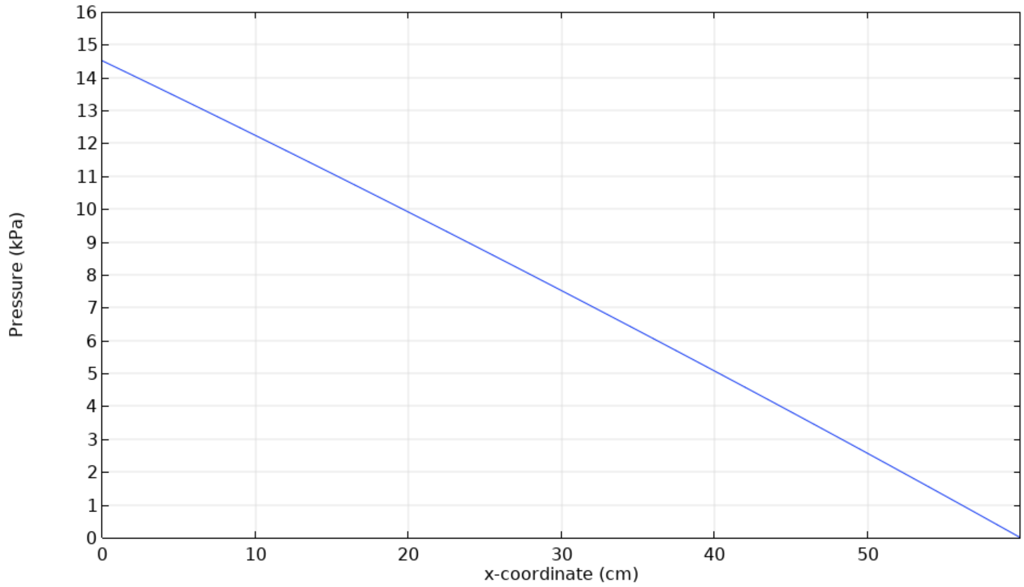

Figure 4.6. Pressure drop along the monolith channel direction for Case 4 (SCR unit diameter: 20 cm, NO conversion target at the end of the channel: 97%)

Required SCR unit lengths and the related pressure drops to obtain 97% and 98% NO conversions are provided in Table 4.4. It is seen that 50% more pressure drop showed up for 1% more NO conversion in this SCR deNOx unit system. Therefore, it seems arguable to keep the conversion at 98% for the SCR system when the additional pressure drop is considered.

Table 4.4. SCR deNO$_x$ unit lengths and pressure drops associated with 97% and 98% NO conversion

Computed in Present Work		
	SCR Unit Length (cm)	**Pressure Drop (kPa)**
97% NO Conversion	60	14.5
98% NO Conversion	115	29.1

In equation (33), it is seen that pressure drop increases when the SCR unit length increases and the results obtained in this section supports this argument. Furthermore, the manufacturer of the reference engine SCANIA recommends 26.5 kPa maximum pressure drop along the entire exhaust system. Results showed that 29.1 kPa pressure drop is observed at Case 4 when 600 cpsi and 20 cm diameter deNO_x unit is utilized. In order to keep the SCR unit length and therefore pressure drop lower while having the same 98% conversion, diameter of the unit can be increased. 115 cm length is required to obtain 98% NO conversion when the SCR system diameter is 20 cm.

4.2.1. Effect of the SCR Unit Diameter

As it is mentioned in Section 2.1.1., monoliths used in heavy duty vehicles can have diameters up to 38 cm today. In the present work, it is observed that using 38 cm diameter for a 600 cpsi monolith is not required since the lengths where 98% NO conversion achieved are not reasonable. Since the previous section enlightened that 20 cm diameter-units requires long SCR units (115 cm for Case 4) to achieve 98% NO conversion which exceeds the manufacturer's recommended pressure drop value (26.5 kPa). To decrease the length of the SCR, diameter of the unit is increased from 20 cm to 25 cm. Increasing the diameter decreases the inlet velocity and increase the catalytic activity since the number of channels increase. Both results have positive impacts on the NO conversion to achieve 98% conversion earlier in the monolith channel direction.

Table 3.4 in Section 3.1.6 represents the inlet velocities calculated at each diameter from 20 cm to 25 cm. In Figure 4.7, it can be observed that lowest inlet velocity (21.6 m/s) arising from the highest diameter (25 cm) provides the earliest achievement of 98% NO conversion. Besides, it is seen that 115 cm length is not required when the diameter is increased since 98% conversion can be obtained much before the 115 cm length.

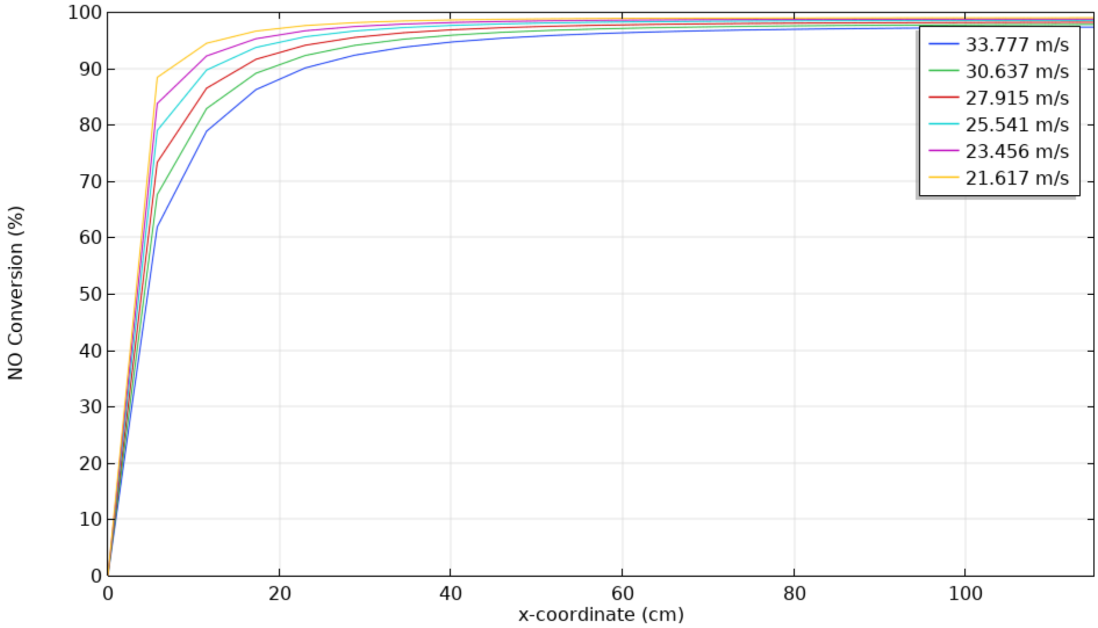

Figure 4.7. NO Conversion along the monolith channel direction for Case 4 at different inlet velocities arising from different diameters (from 20 cm up to 25 cm)

Figure 4.8. demonstrates that the lowest inlet velocity gives the best result in backpressure aspect. However, the actual pressure drops are even less since the 98% conversion can be obtained much before the complete 115 cm length.

Figure 4.9 and Figure 4.10 represent that 25 cm diameter SCR geometry gives the best results among the other diameter trials since it gives the lowest backpressure due to lowest inlet velocity and highest catalytic activity. However, it might be a further discussion that the SCR with the lowest length can age earlier since the reactive monolith channels will lose their catalytic activity with time because of the deposition occurring on the catalyst surface. Thus, it might be better if the balance between the pressure drop and the length of the monolith is regarded.

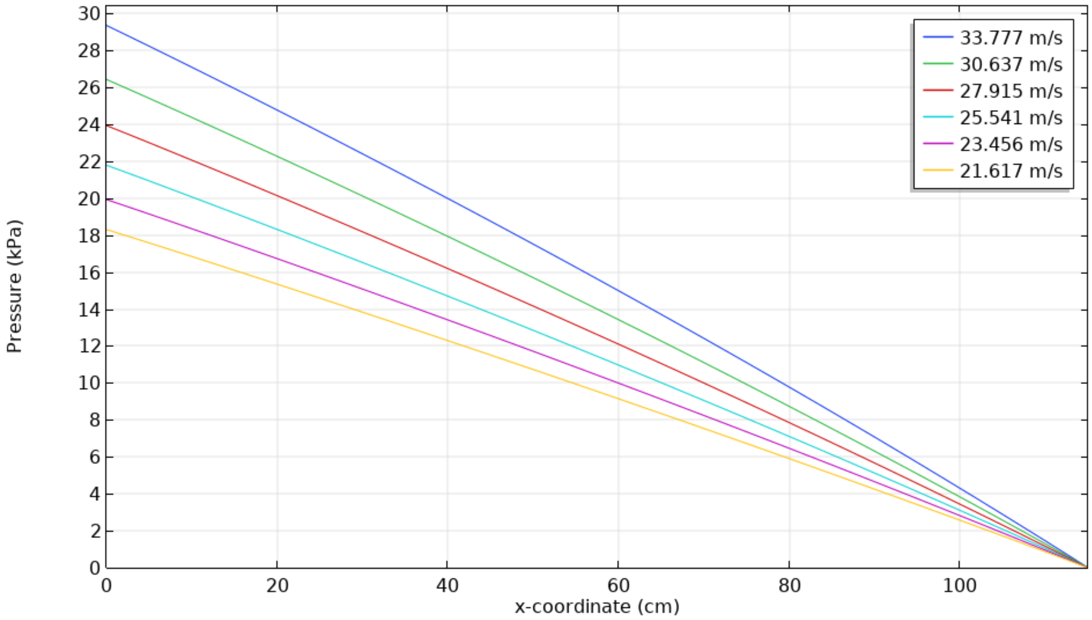

Figure 4.8. Pressure along the monolith channel direction for Case 4 at different inlet velocities arising from different diameters (from 20 cm up to 25 cm)

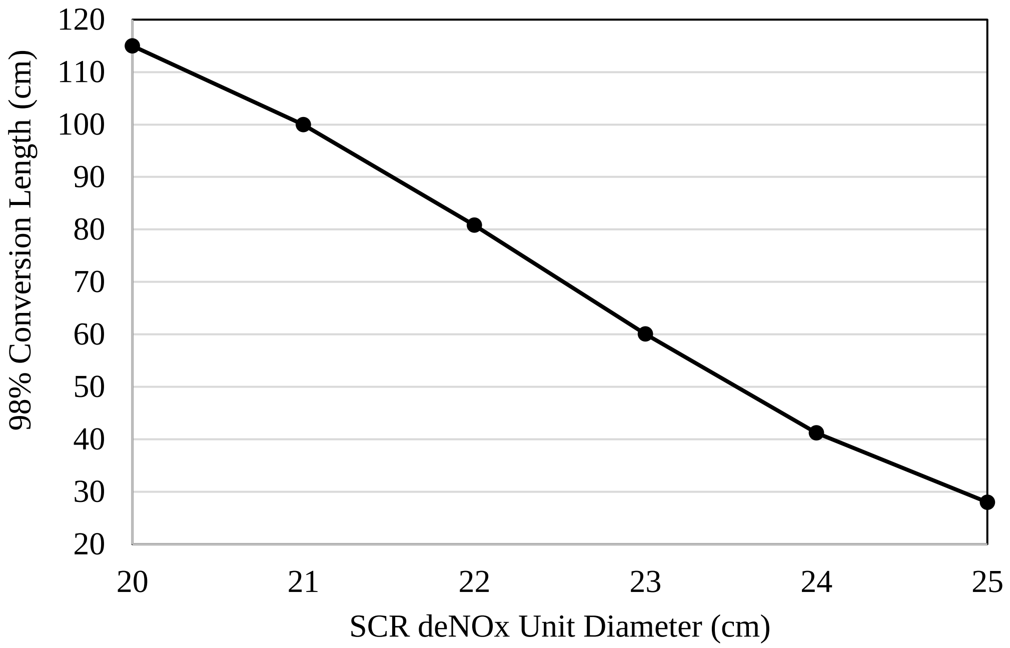

Figure 4.9. Variation of the lengths for Case 4 where 98% NO conversion achieved with increasing SCR unit diameter

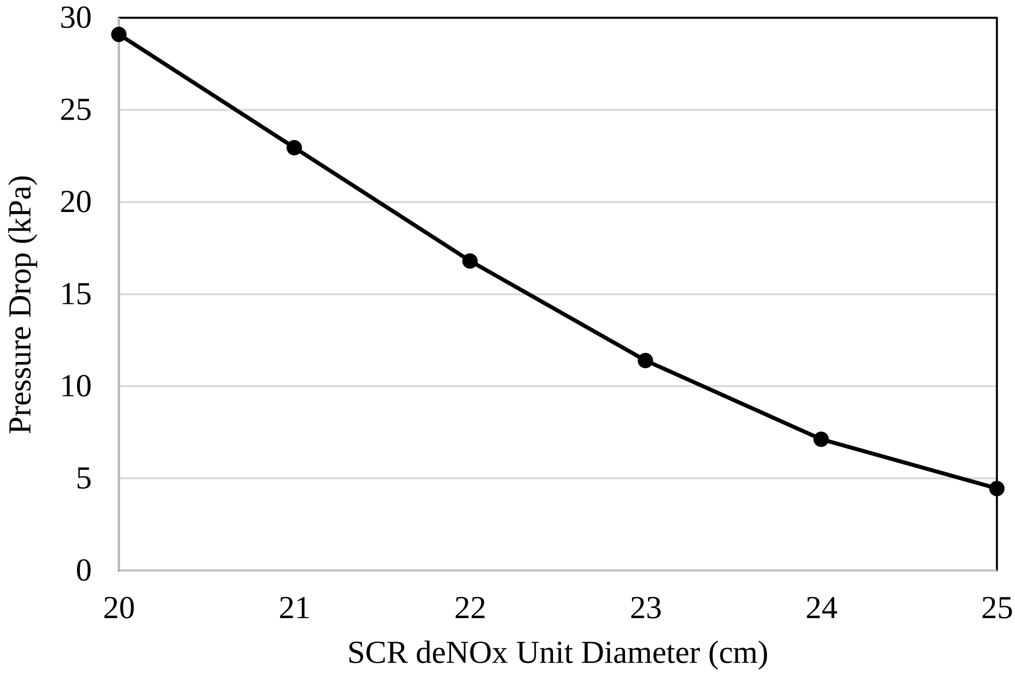

Figure 4.10. Pressure drop variation for Case 4 with increasing SCR unit diameter

4.2.2. Effect of the SCR Inlet Temperature

The results are obtained for the different inlet temperatures by keeping the inlet velocity and the SCR geometry constant to observe the effect of the inlet temperature on the SCR process. Temperature values are from 300 K to 700 K with 100 K increment. SCR $deNO_x$ unit length and diameter are taken as 100 cm and 20 cm respectively.

Since the reaction rate depends upon the temperature, it is expected that the conversion characteristic increase with the increasing temperature for the rate mechanism used in this work. As it is observed in Figure 4.11, the SCR system operates more efficient in 600 and 700 K temperatures whereas it does not work sufficiently for the temperatures closer to atmospheric temperature which are 300 K and 400 K.

Darcy Law is considered while examining the pressure drop results. In this section, the inlet velocity and outlet pressure are kept constant to observe the inlet temperature effect. Therefore, the reason behind why higher temperature causes higher pressure drop is that the dynamic viscosity changing with the temperature. (See Figure 4.12)

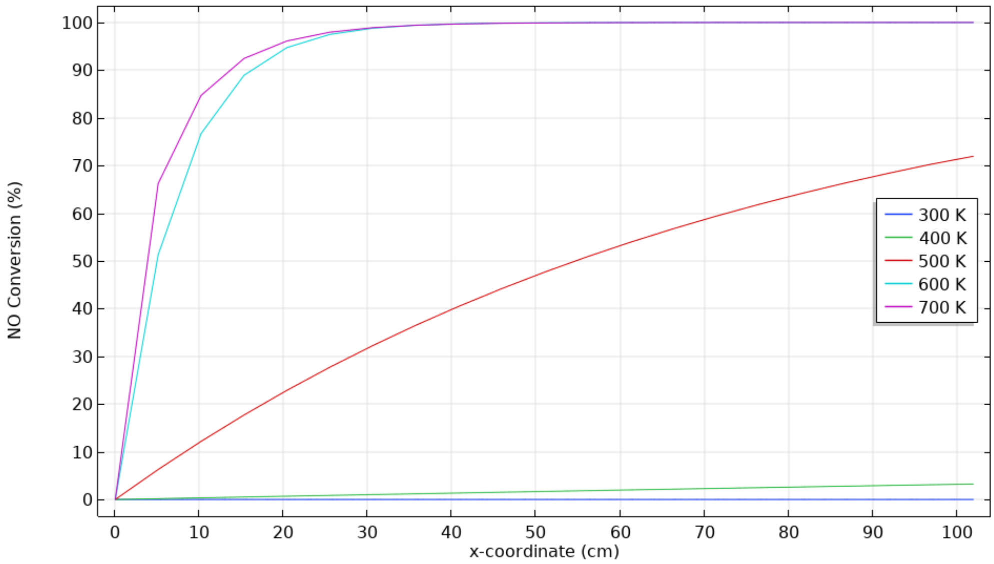

Figure 4.11. NO Conversion along the monolith channel direction by using exhaust mass flow rate of Case 4

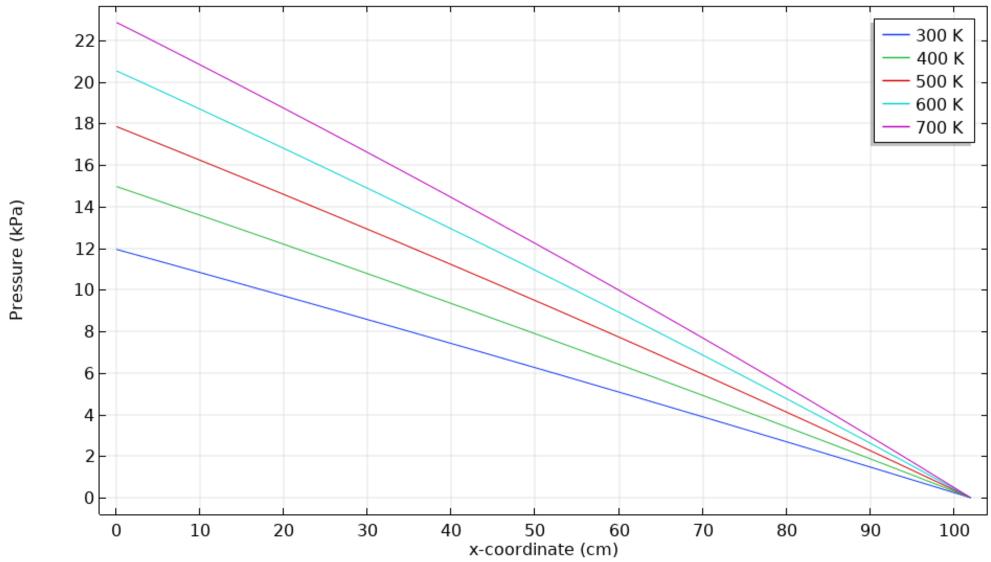

Figure 4.12. Pressure drop along the monolith channel direction by using exhaust mass flow rate of Case 4

Since the pressure drop in 700 K is higher, velocity is supposed to increase along the channel (x direction) due to Darcy Law as it is observed in Figure 4.13.

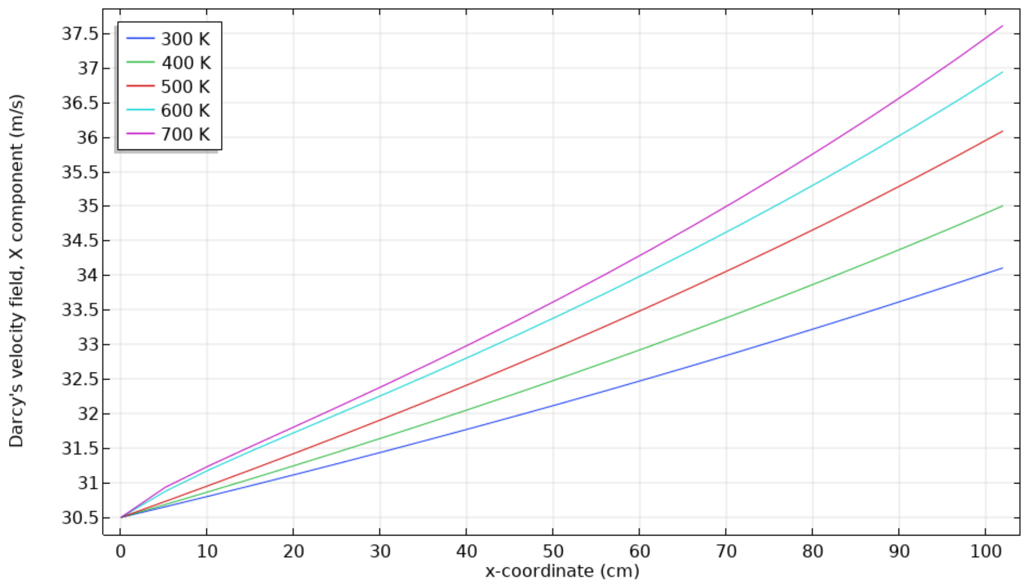

Figure 4.13. Darcy velocity along the monolith channel direction by using exhaust mass flow rate of Case 4

There is almost no temperature change along the monolith channel as it is seen in Figure 4.14. Temperature increases due to heat of exothermic SCR reaction but since NO and NH_3 concentrations are very low in the inlet gas mixture, the temperature increase is negligible. There studies in the literature that SCR unit is assumed isothermal while performing modeling activities [45, 46].

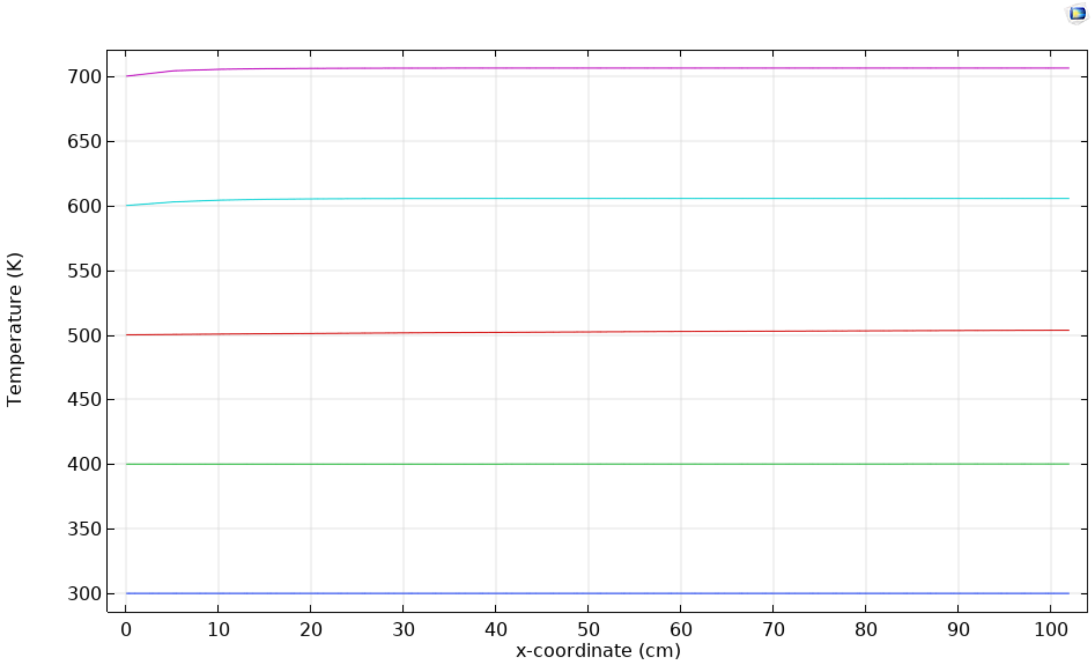

Figure 4.14. Temperature along the monolith channel direction by using exhaust mass flow rate of Case 4

4.3. Thermodynamic Analysis Results

Keeping the other parameters constant, increasing compression ratio increases net work and therefore the efficiency of the engine increases. However, NO_x emission increases with the increasing compression ratio as it is obtained from the result of various published sources mentioned in Section 2.2.2.3.

Maximum backpressure is observed at case 4 for the reference engine and it is 29.1 kPa. When this pressure drop is plugged into thermal efficiency equation and ideal Diesel cycle analysis is performed, the results in the Table 4.5 are obtained. Compression ratio and cut-off ratios are assumed 20 and 2.9 respectively.

Table 4.5. Ideal Diesel cycle efficiency results with and without pressure drop

	Without SCR backpressure	**With SCR backpressure**
Cut-off ratio r_c	2.9	2.9
Compression ratio r	20	18.8
Ideal thermal efficiency η	61%	60%

It is observed that the thermal efficiency calculations based on ideal Diesel cycle are much higher than the actual ones taken from the literature. However, the decrease trend can be observed by performing ideal cycle analysis as well.

29.1 kPa pressure drop caused 1% efficiency loss with the decrease of compression ratio when the maximum cylinder pressure and heat addition are kept constant. On the other hand, decrease in the cylinder stroke size provides better results for the system weight and volume.

CHAPTER 5

CONCLUSION

5.1. Summary

Emission control has become more important for vehicles in recent years due to the fact that the latest emission regulations introduce stricter NO_x emission targets. SCR is one of the most efficient NO_x emission control methods providing high NO_x conversion. However, use of SCR element in exhaust systems raises backpressure issue inevitably. Engine followed by an SCR unit requires to have higher exit pressure to overcome the resistance caused by the exhaust equipment and vent the exhaust gas to the atmosphere.

In the present work, backpressure caused by SCR deNO_x units is assessed in several aspects. Commonly used SCR deNO_x units in the market are investigated in terms of geometry regarding cell density, length, diameter and channel shapes. It is obtained that the SCR deNO_x units with 300-400 cpsi are used mostly. Additionally, diameters of the unit can be up to 38 cm for heavy duty vehicles [40]. In the present study, a monolith geometry with 600 cpsi cell density is used to examine an SCR unit different than commonly used in the market. Latest declared NO_x limits drive this study to use a SCR with higher cell density which is supposed to have a higher catalytic activity due to increased catalyst surface. The existing 3D monolith reactor model in COMSOL Multiphysics® applications is modified to account for an SCR deNO_x unit having 600 cpsi cell density by using exhaust mass flow rate and temperature data of a SCANIA 9-liter off-road Diesel engine. The model is verified against a published experimental work [32]. While performing the analysis, %98 NO_x conversion is aimed since this conversion target provides the best results in terms of system cost, fuel consumption and the elimination of EGR and apply SCR only [40]. Obtained backpressure values are compared with maximum backpressure recommended by the engine manufacturer. SCANIA, which is the manufacturer of the engine used in the present study, recommends 26.5 kPa maximum pressure drop along the entire exhaust system [10].

5.2. Conclusion

Results of this modeling study showed that 29.1 kPa backpressure is observed at 2100 rpm engine speed when 600 cpsi and 20 cm diameter deNO_x unit is utilized. The result is higher than the recommended pressure despite this backpressure represents SCR unit only. Therefore, keeping the cell density constant at 600 cpsi, diameter of the deNO_x unit is increased in order to decrease catalyst length and pressure drop while obtaining better catalyst performance. It is observed that pressure drop decreased down to 4.9 kPa by increasing the diameter to 25 cm. Besides, 98% conversion can be obtained at an earlier length when 25 cm diameter unit is used. This also provides weight and volume saving for the SCR system.

Furthermore, it is observed that 50% more backpressure occurs in order to gain only 1% more NO_x conversion (from 97% to 98%) in the examined SCR conditions. Hence, it seems arguable to aim 98% NO conversion for the SCR system when the additional backpressure is considered. On the other hand, catalysts age with time. Therefore, providing extra length to the catalyst element might be good for its maintenance and life cycle costs.

In thermodynamic analysis, compression ratio parameter is selected to sight the engine efficiency along with the NO_x emission. An engine designed with higher compression ratio has a higher net work. Thus, the efficiency of the engine increases and the fuel consumption decreases. At the same time, CO_2 emission decreases since it is directly related to amount of the fuel consumed. In contrast to CO_2 emission, NO_x emission increases with the increasing compression ratio. An ideal cycle is examined aiming a higher engine exhaust pressure to overcome aftertreatment resistance while decreasing the compression ratio in order to obtain less NO_x emission by being aware of that the engine efficiency will decrease. As a result, 29.1 kPa backpressure caused 1%

efficiency loss for an ideal cycle. On the other hand, decrease in the cylinder stroke size provides better results for the system weight and volume. Results also revealed that the engine and aftertreatment equipment shall be designed so that they can operate accordantly in order to optimize fuel consumption and NO_x emission parameters.

5.3. Future Work

In the present work, only 600 cpsi cell density geometry is used for backpressure calculations, the effect of the other cell densities used in automotive applications (from 25 cpsi to 900 cpsi) can be also examined in backpressure and NO_x conversion aspects.

The type of washcoat used in the present work is Vanadia-Titania. In order to observe the internal mass transfer effects, other catalyst type might be used in a future work such as metal-exchanged zeolites.

Required SCR unit lengths and the related pressure drops to obtain 97% and 98% NO conversions are provided in Table 4.2. It is seen that 50% more pressure drop obtained for 1% more NO conversion in this SCR deNO_x unit system. Hence, it seems arguable to keep the conversion at 98% for the SCR system when the additional pressure drop is considered. On the other hand, catalysts become aged with time thus providing extra length to the catalyst is good for its maintenance and life cycle. In a future work, the aging characteristics of the catalyst unit can be investigated and it might be a decent input to this study.

Finally, further thermodynamic analyses can be performed for Diesel engines considering SCR backpressures. More reasonable results in engine efficiency can be obtained by using various softwares and detailed engine data.

REFERENCES

[1] Brandenberger, S., Kröcher, O., Tissler, A., & Althoff, R. (2008). The State of the Art in Selective Catalytic Reduction of NOx by Ammonia Using Metal-Exchanged Zeolite Catalysts. Catalysis Reviews, 50(4), 492–531. doi:10.1080/01614940802480122

[2] Non-Renewable Resources. (2019). Retrieved 8 December 2019, from https://www.tiredearth.com/news/non-renewable-resources

[3] New EU rules for lower power plant emissions take effect. (2019). Retrieved 8 December 2019, from https://www.euractiv.com/section/air-pollution/news/new-eu-rules-for-lower-power-plant-emissions-take-effect/

[4] James Nix: Volkswagen crisis provides pretext for overdue rise in tax on Diesel |. (2019). Retrieved 8 December 2019, from https://green-budget.eu/james-nix-volkwagen-crisis-provides-pretext-for-overdue-rise-in-tax-on-Diesel/

[5] Clark, C. (2019). NOx Abatement - Gulf Coast Environmental Systems. Retrieved 8 December 2019, from http://www.gcesystems.com/nox/

[6] Kampa, M., & Castanas, E. (2008). Human health effects of air pollution. Environmental Pollution, 151(2), 362–367. doi: 10.1016/j.envpol.2007.06.012

[7] Nitrogen Oxides (NOx) Emissions | netl.doe.gov. (2019). Retrieved 8 December 2019, from https://www.netl.doe.gov/research/Coal/energy-systems/gasification/gasifipedia/nitrogen-oxides

[8] Richards, J. (2000). Control of Nitrogen Oxides Emissions, Student Manual, APTI Course 418. NC: Air Pollution Training Institute (APTI). Retrieved from http://www.4cleanair.org/APTI/418Combinedchapters.pdf

[9] Emission Standards. (2019). Retrieved December 10, 2019, from https://www.Dieselnet.com/standards/.

[10] SCANIA. (2018). Exhaust system, industrial engines DC09, DC13, DC16: Installation manual. Sweden.

[11] Williams, M., & Minjares, R. (2016). A technical summary of Euro 6/Vi vehicle emission standards. A technical summary of Euro 6/VI vehicle emission standards. The International Council of Clean Transportation.

[12] Regulation (EC) No. 715/2007 of the European Parliament and of the Council, Official Journal of the European Union, L 171/1, Retrieved June 29, 2007, from http://eurlex.europa.eu/LexUriServ/LexUriServ.do?uri=OJ:L:2007:171:0001:0016:EN:PDF.

[13] V. Praveena, M.L.J. Martin, A Review on Various After Treatment Techniques to Reduce NOx emissions in a CI Engine, Journal of the Energy Institute (2017), doi: 10.1016/ j.joei.2017.05.010.

[14] Amirnordin, S. H., Seri, S. M., Salim, W. S.-I. W., Rahman, H. A., & Hasnan, K. (2011). Pressure Drop Analysis of Square and Hexagonal Cellsand its Effects on the Performance of Catalytic Converters. International Journal of Environmental Science and Development, 239–247. doi: 10.7763/ijesd.2011.v2.131

[15] Fonseca González, N., Casanova Kindelán, J., & López Martí;nez, J. M. (2016). Methodology for instantaneous average exhaust gas mass flow rate measurement. Flow Measurement and Instrumentation, 49, 52–62. doi:10.1016/ j.flowmeasinst.2016.04.007

[16] Ferguson, C. R., & Kirkpatrick, A. T. (2001). Internal combustion engines: applied thermodynamics. New Delhi, India: John Wiley & Sons, Inc.

[17] Mollenhauer, K., Tschoeke, H., & Johnson, K. G. E. (2010). Handbook of Diesel engines. Heidelberg: Springer.

[18] Çağlar, B. (2009) NOx storage and reduction over Ce-Zr mixed oxide supported catalyst. (Unpublished master dissertation). Middle East Technical University, Ankara, Turkey

[19]Multiphase Catalytic Reactors: Theory, Design, Manufacturing, and Applications. (2016). New York: John Wiley & Sons.

[20] Raberger, N. B., Stutz, M. J., Hotz, N., & Poulikakos, D. (2009). Simulation of the Postcombustor for the Treatment of Toxic and Flammable Exhaust Gases of a

Micro-Solid Oxide Fuel Cell. Journal of Fuel Cell Science and Technology,6(4), 041002. doi:10.1115/1.3080812

[21] Beeckman, J. W., & Hegedus, L. L. (1991). Design of monolith catalysts for power plant nitrogen oxide (No. -.) emission control. Industrial & Engineering Chemistry Research,30(5), 969-978. doi:10.1021/ie00053a020

[22] Dumesic, J., Topsøe, N., Topsøe, H., Chen, Y., & Slabiak, T. (1996). Kinetics of Selective Catalytic Reduction of Nitric Oxide by Ammonia over Vanadia/Titania. Journal of Catalysis,163(2), 409-417. doi:10.1006/jcat.1996.0342

[23] Baharudin, L., & Watson, M. J. (2018). Erratum to: Monolithic substrate support catalyst design considerations for steam methane reforming operation. Reviews in Chemical Engineering,34(5), 741-741. doi:10.1515/revce-2018-9001

[24] Crittenden, B., Perera S. (2005) Monolithic adsorbents in sustainable development. Industrial & Engineering Chemistry Research,30(5), 969-978

[25] Sher, E. (1998). Handbook of air pollution from internal combustion engines: pollutant formation and control. Boston: Academic Press.

[26] Stone, R. (2012). Introduction to internal combustion engines. Houndmills: MacMillan Press.

[27] Kurre, S., Pandey, S. (2013). Effect of Compression Ratio on Diesel Engine Performance and Emission with Diesel-Ethanol Blends. International Journal of Scientific and Engineering Research

[28] Raheman, H., & Ghadge, S. V. (2008). Performance of Diesel engine with bioDiesel at varying compression ratio and ignition timing. Fuel, 87(12), 2659–2666. doi:10.1016/j.fuel.2008.03.006

[29] Vasudeva, M., Sharma, S., Mohapatra, S. K., & Kundu, K. (2016). Performance and exhaust emission characteristics of variable compression ratio Diesel engine fuelled with esters of crude rice bran oil. SpringerPlus, 5(1). doi: 10.1186/s40064-016-1945-7

[30] Hirkude, J., & Padalkar, A. S. (2014). Experimental investigation of the effect of compression ratio on performance and emissions of CI engine operated with waste

fried oil methyl ester blend. Fuel Processing Technology, 128, 367–375. doi:10.1016/j.fuproc.2014.07.026

[31] Jindal, S., Nandwana, B. P., Rathore, N. S., & Vashistha, V. (2010). Experimental investigation of the effect of compression ratio and injection pressure in a direct injection Diesel engine running on Jatropha methyl ester. Applied Thermal Engineering, 30(5), 442–448. doi:10.1016/j.applthermaleng.2009.10.004

[32] COMSOL: Multiphysics Software for Optimizing Designs. (n.d.). Retrieved from https://www.comsol.com/.

[33]Cansu Ozhan. Multi-scale simulation of automotive catalytic converters. Mechanics of the fluids [physics.class-ph]. Université Pierre et Marie Curie - Paris VI, 2014. English. ffNNT : 2014PA066484ff. fftel-01232031f

[34]Williams, J. L. (2001). Monolith structures, materials, properties and uses. Catalysis Today, 69(1-4), 3–9. doi:10.1016/s0920-5861(01)00348-0

[35] Cordierite ceramic monolith catalytic converter substrate. (n.d.). Retrieved from https://www.ceramictek.com/alumina-ceramic-substrate/54414518.html

[36] G. Schaub, D. Unruh, J. Wang, and T. Turek, "Kinetic analysis of selective catalytic NOx reduction (SCR) in a catalytic filter," Chemical Engineering and Processing, vol. 42, no. 3, pp. 365–371, 2003.

[37] ENGINES. (n.d.). Retrieved from https://www.scania.com/global/en/home/products-and-services/engines/our-range/industrial-engines.html.

[38] Gardiner, W. C. (1984). Combustion chemistry. Berlin u.a.: Springer.

[39] (n.d.). Retrieved from https://www.ozonelayer.noaa.gov/science/basics.htm.

[40] SPRINGER. (2014). Urea-scr technology for denox after treatment of Diesel exhausts.

[41] Changes in Automobile Control System To Accommodate EURO 6(n.d.). Retrieved from https://www.researchgate.net/profile/Yaswanth_Dontu/publication/264727124_Changes_in_Automobile_Control_System_To_Accommodate_EURO_6_Emission_Standards/links/53ecc0d30cf2981ada10dddf/Changes-in-Automobile-Control-System-To-Accommodate-EURO-6-Emission-Standards.pdf?origin=publication_detail

[42] Heibel, A. (2010) Advances in Substrate Technology, presentation at SAE Heavy-Duty Diesel Emissions Control Symposium, Gothenburg, September 2010.

[43] Stanton, D. (2012) Diesel Engine Technologies to Meet Future On-Road and Off-Road US EPA Regulations, presentation at 4th CTI International Conference, NOx Reduction, Current and Future Solutions for On-Road and Off-Road Applications, Detroit, June 19–20, 2012.

[44] Roberts, C. (2011) The Pursuit of High Efficiency Engines-SwRI Programs, presentation at the Emissions 2011 Conference, Ann Arbor, MI, June 2011.

[45] Metkar, P. S., Balakotaiah, V., & Harold, M. P. (2011). Experimental study of mass transfer limitations in Fe- and Cu-zeolite-based NH3-SCR monolithic catalysts.Chemical Engineering Science,66(21),5192–5203. doi:10.1016/ j.ces.2011.07.014

[46] Goldbach, M., Roppertz, A., Langenfeld, P., Wackerhagen, M., Füger, S., & Kureti, S. (2017). Urea Decomposition in Selective Catalytic Reduction on V2 O5 /WO3 /TiO2 Catalyst in Diesel Exhaust. Chemical Engineering & Technology, 40(11), 2035–2043. doi:10.1002/ceat.201700261

[47] Joshi, S. Y., Harold, M. P., & Balakotaiah, V. (2010). Overall mass transfer coefficients and controlling regimes in catalytic monoliths. Chemical Engineering Science, 65(5), 1729–1747. doi:10.1016/j.ces.2009.11.021

[48] Domkundwar, V.M., 2000. A Course in Internal Combustion Engine. Dhanpat Rai and CO. (P) Ltd.

[49] Hield, P. (2011). The Effect of Backpressure on the Operation of Diesel Engines. Maritime Platform Division, Defense Science and Technology Organization, Australian Government (Unclassified): DSTO-TR-2531.

[50] Cong, S., Garner, C. P., & McTaggart-Cowan, G. P. (2011). The Effects of Exhaust Back Pressure on Conventional and Low-Temperature Diesel Combustion. Proceedings of the Institution of Mechanical Engineers, Part D: Journal of Automobile Engineering, 225(2), 222–235. doi:10.1177/09544070jauto1577

[51] Burnete, N., Moldovanu, D., Baldean, D. L., & Kocsis, L. (2016). Studies Regarding the Influence of Exhaust Backpressure on the Performances of a Compression Ignited Engine, in Proc. of the European Automotive Congress EAEC-ESFA 2015, November 2015, 141-149.

[52] Fox, R. W., McDonald, A. T., Pritchard, P. J., Mitchell, J. W., & Leylegian, J. C. (2016). Fluid mechanics. Hoboken, NJ: Wiley.

[53] Hawthorn, R.D.; "Afterburner catalysts- Effect of heat and mass transfer between gas and catalyst surface", AICHE Symp. Series, SHELL DEVELOPMENT

[54] Shah, R.K.; "A correlation for laminar hydrodynamic entry length solutions for circular and non-circular ducts", Transactions of the ASME, Journal of fluids engineering, vol. 100, pp. 177-179, June 1978.

[55] Abu-Khiran, E., Douglas, R., & Mccullough, G. (2003). Pressure Loss Characteristics in Catalytic Converters. SAE Technical Paper Series. doi: 10.4271/2003-32-0061

[56] Balakotaiah, V. (2008). On the relationship between Aris and Sherwood numbers and friction and effectiveness factors. Chemical Engineering Science, 63(24), 5802–5812. doi:10.1016/j.ces.2008.08.025

APPENDICES

APPENDIX A

Exhaust mass flow rate and exhaust temperatures data of a 9-liter 202 kW SCANIA off-road engine at different engine speeds are used in NO conversion and pressure drop calculations. Four cases stated in Table 4.3 are examined. Results obtained for Case 1, Case 2 and Case 3 are represented in this section while the result of Case 4 is involved in the main body of the study since this case gives the highest backpressure result and therefore found more critical.

Case 1

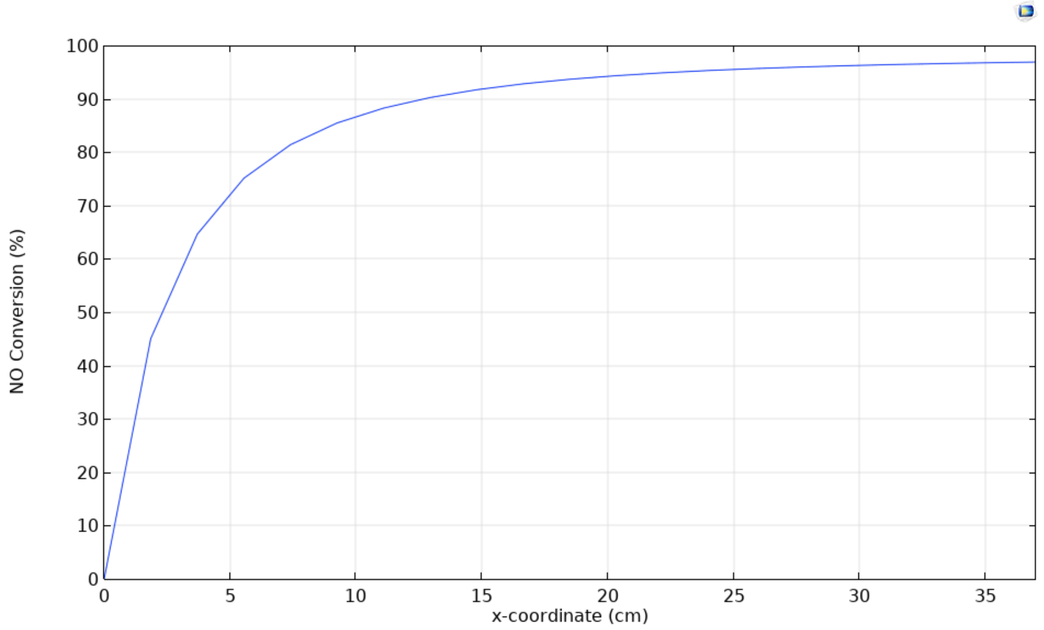

Figure 7.1. NO conversion along the monolith channel direction for Case 1 (SCR unit diameter: 20 cm, NO conversion target at the end of the channel: 98%)

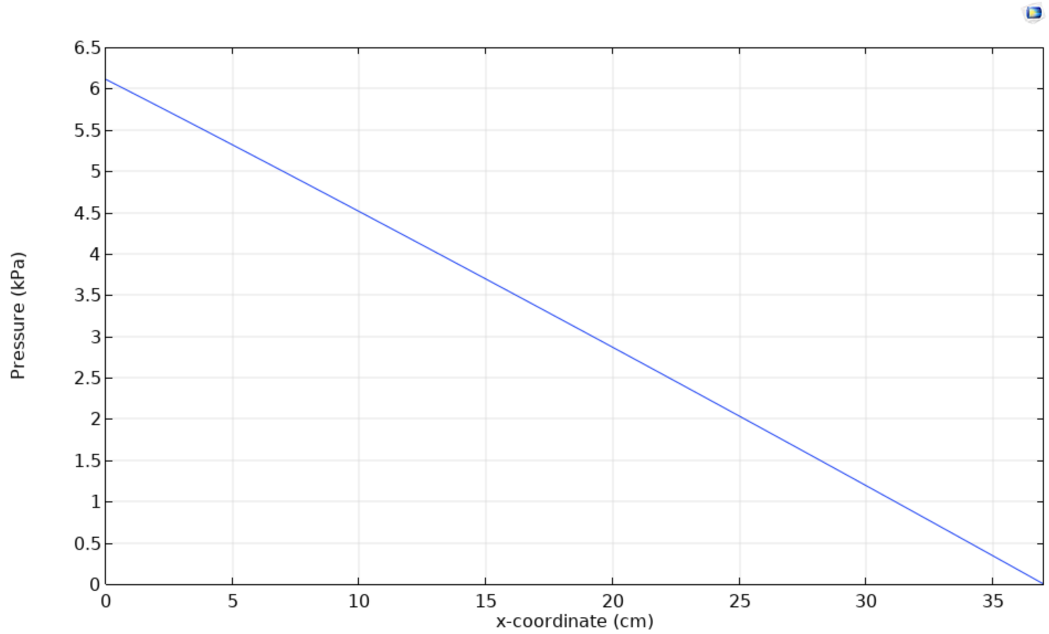

Figure 7.2. Pressure drop along the monolith channel direction for Case 1 (SCR unit diameter: 20 cm, NO conversion target at the end of the channel: 98%)

Case 2

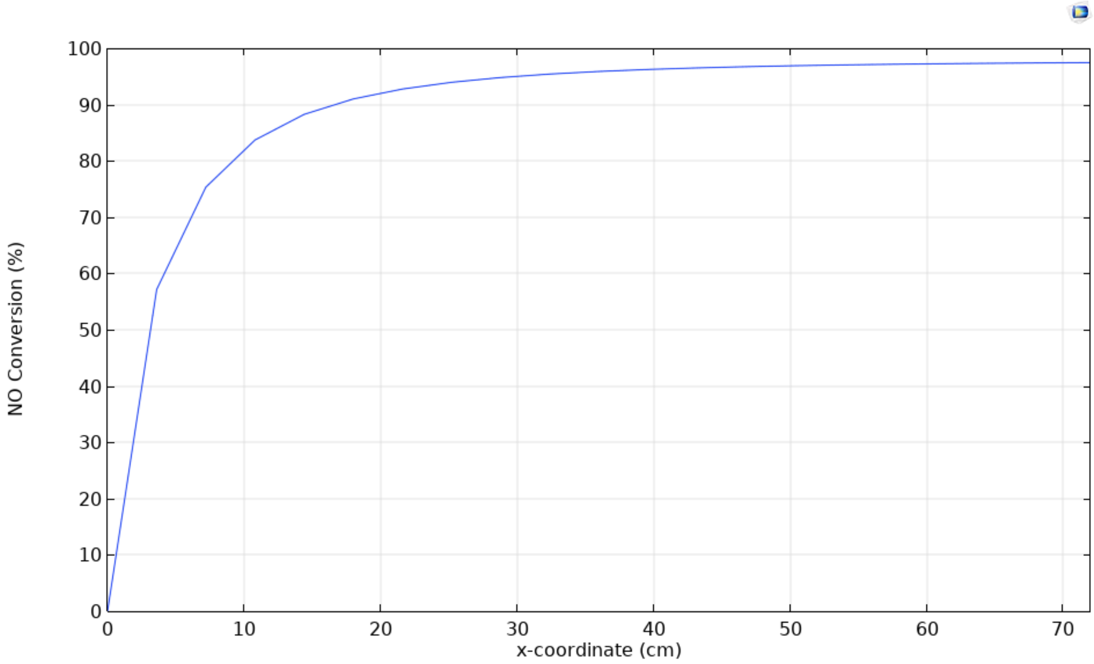

Figure 7.3. NO conversion along the monolith channel direction for Case 2 (SCR unit diameter: 20 cm, NO conversion target at the end of the channel: 98%)

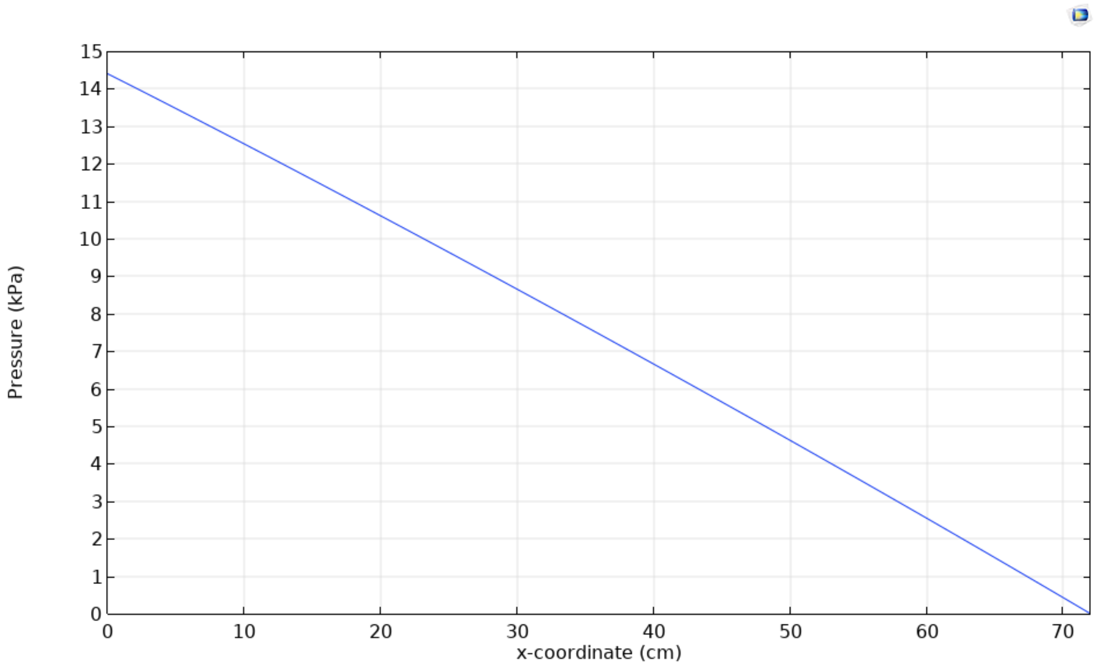

Figure 7.4. Pressure drop along the monolith channel direction for Case 2 (SCR unit diameter: 20 cm, NO conversion target at the end of the channel: 98%)

Case 3

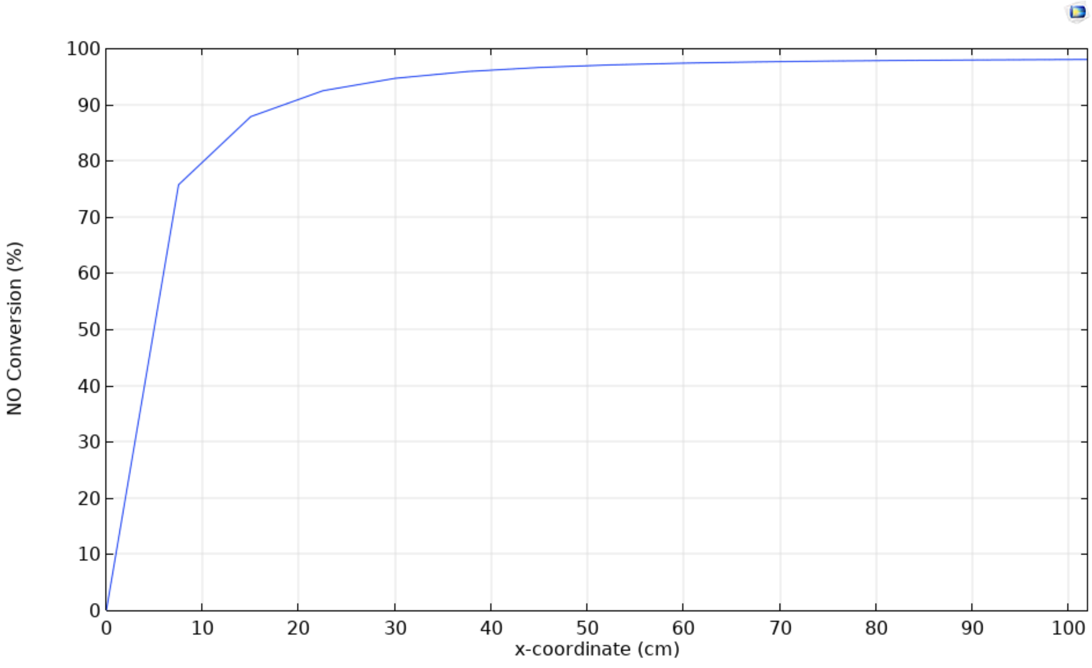

Figure 7.5. NO conversion along the monolith channel direction for Case 3 (SCR unit diameter: 20 cm, NO conversion target at the end of the channel: 98%)

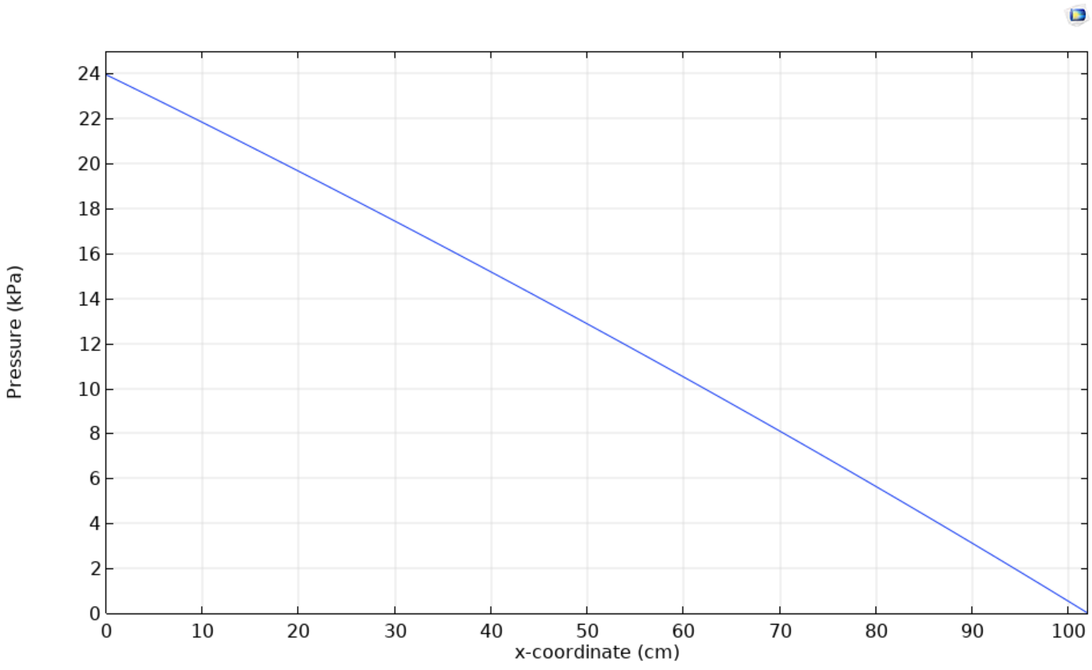

Figure 7.6. Pressure drop along the monolith channel direction for Case 3 (SCR unit diameter: 20 cm, NO conversion target at the end of the channel: 98%)